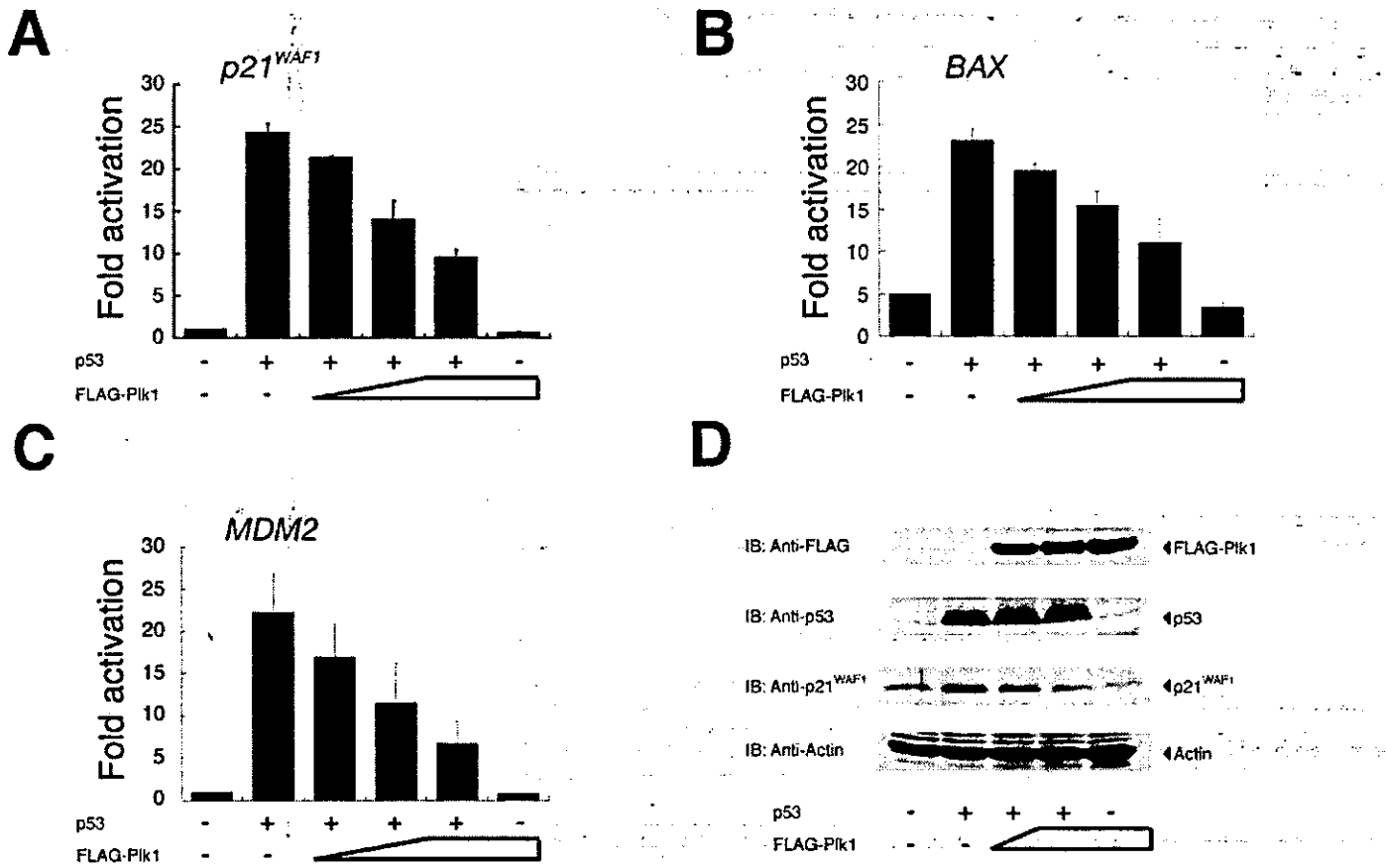

FIG. 6. **Plk1 abrogates the p53-mediated transcriptional activation.** *p53*-deficient H1299 cells (5×10^4 cells/well) were transiently co-transfected with 25 ng of the expression plasmid for p53 together with 100 ng of the luciferase reporter construct that carries the p53-responsive element derived from $p21^{WAF1}$ (*A*), *BAX* (*B*), or *MDM2* (*C*) promoter and 10 ng of the *Renilla* luciferase plasmid (pRL-TK) in the presence or absence of increasing amounts of pcDNA3-FLAG-Plk1 (50, 100, or 200 ng). The total amount of plasmid DNA per transfection was kept constant (510 ng) with pcDNA3. All transfections were performed in triplicate. Forty-eight hours after transfection, cells were lysed, and analyzed for their luciferase activities. Firefly luminescence signal was normalized based on the *Renilla* luminescence signal. Results are shown as -fold induction of the firefly luciferase activity compared with control cells transfected with pcDNA3 alone. *D*, immunoblot analysis. H1299 cells were transiently co-transfected with the indicated combinations of expression plasmids. Whole cell lysates were prepared 48 h post-transfection, and analyzed for the expression of FLAG-Plk1 (*1st panel*), p53 (*2nd panel*), or $p21^{WAF1}$ (*3rd panel*) by immunoblot analysis with monoclonal anti-FLAG, monoclonal anti-p53, or polyclonal anti-$p21^{WAF1}$ antibody, respectively. Total protein levels were controlled with polyclonal anti-actin antibody (*4th panel*).

nous $p21^{WAF1}$. To this end, H1299 cells were transiently co-transfected with a constant amount of the expression plasmid for p53 together with or without increasing amounts of the FLAG-Plk1 expression plasmid. Forty-eight hours after transfection, whole cell lysates were prepared and subjected to immunoblot analysis. Equal protein loading was confirmed by immunoblotting with the antibody against actin. As described (46), overexpression of p53 in H1299 cells resulted in the induction of the endogenous $p21^{WAF1}$ compared with basal levels seen with empty plasmid (Fig. 6*D*, *first* and *second lanes*). Co-expression of p53 with FLAG-Plk1 caused a significant decrease in the endogenous $p21^{WAF1}$ level in a dose-dependent manner (Fig. 6*D*, *third* and *fourth lanes*). These findings strongly suggest that Plk1 has an ability to inhibit p53-mediated transcriptional activation through physical interaction with p53.

To assess the possible effect of the endogenous Plk1 on the transcriptional activity of p53, we have employed an antisense strategy. As shown in Fig. 7*A*, expression of antisense *Plk1* in H1299 cells resulted in a reduction of the endogenous Plk1 as detected by immunoblot analysis. We then performed luciferase reporter analysis utilizing H1299 cells. As expected, co-expression of p53 with the antisense *Plk1* led to a slight but significant increase in the p53-mediated transcriptional activation as compared with cells expressing p53 alone (Fig. 7, *B–D*).

Plk1 Inhibits the p53-mediated Apoptosis—To extend the functional significance of the physical interaction between Plk1 and p53, we next determined whether Plk1 could affect p53-mediated apoptosis. H1299 cells were transiently co-transfected with the expression plasmid encoding p53 together with or without the expression plasmid for FLAG-Plk1. Forty-eight hours after transfection, cell viability was monitored by a cell survival assay. As shown in Fig. 8*A*, overexpression of p53 resulted in a reduction of the number of viable cells as compared with that found in the control transfection, and Plk1 alone had little effect on cell viability. The reduced number of viable cells caused by exogenous p53 was recovered by co-expression of FLAG-Plk1. Considering that p53 induced apoptosis in transfected H1299 cells (47), Plk1 might abrogate the pro-apoptotic function of p53. To confirm this possibility, H1299 cells were transiently co-transfected with a constant amount of the GFP expression plasmid together with the indicated combinations of the expression plasmids. Forty-eight hours after transfection, transfected cells were scored by fluorescence microscopy for the appearance of green fluorescence,

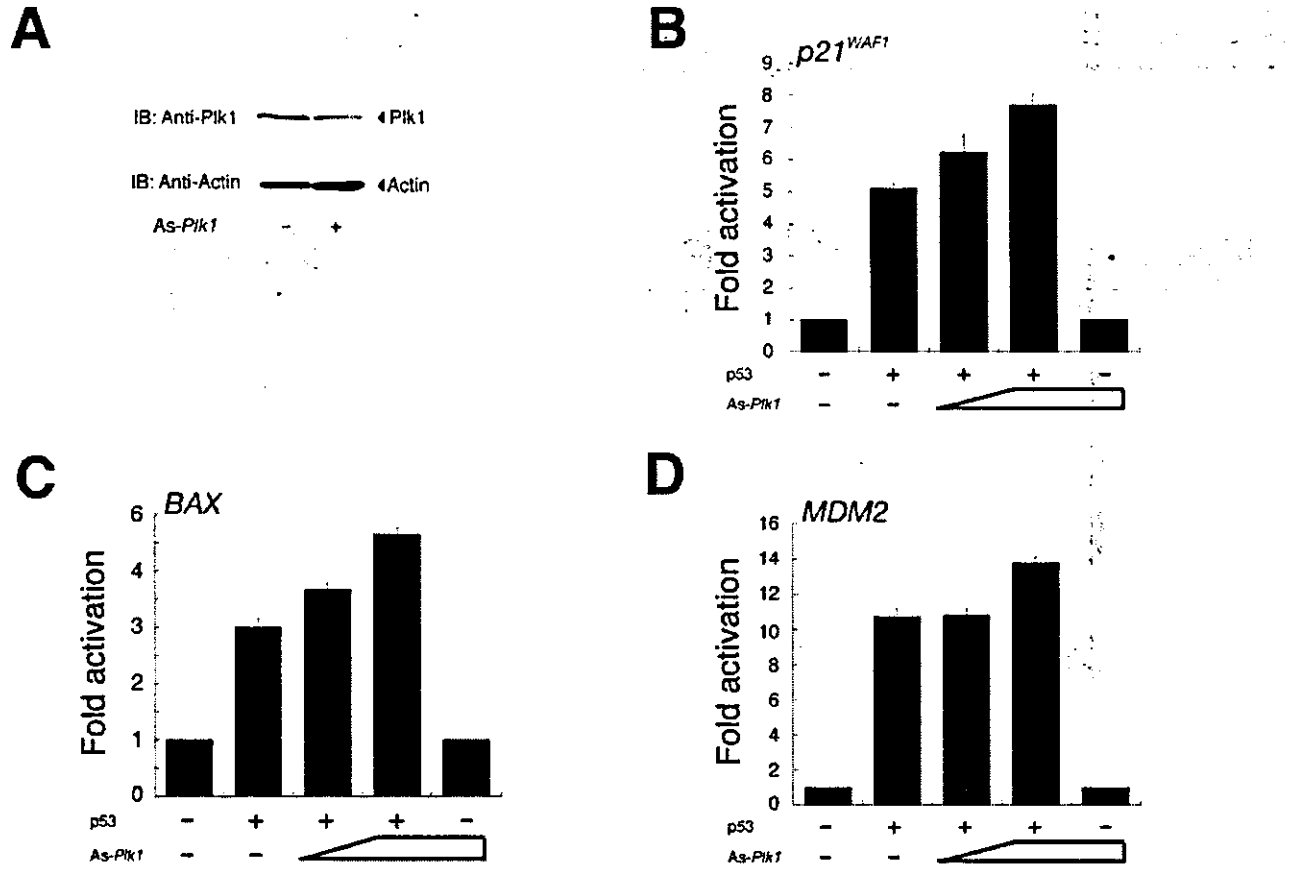

FIG. 7. **Antisense *Plk1* increases the transcriptional activity of p53.** *A*, antisense *Plk1* expression in H1299 cells results in a reduction of endogenous Plk1. H1299 cells were transfected with 2 μg of antisense *Plk1* expression plasmid (*As-Plk1*). Whole cell lysates prepared from transfected cells were subjected to immunoblotting with the anti-Plk1 antibody (*top panel*). Western blotting for actin is shown as a control for protein loading (*bottom panel*). *B–D*, luciferase reporter analysis. H1299 cells were transiently co-transfected with 12.5 ng of the p53 expression plasmid along with 100 ng of the indicated luciferase reporter construct in the presence or absence of increasing amounts of As-*Plk1* (200 and 400 ng). Determination and calculation of the luciferase activities are described in the legend to Fig. 6.

and the number of GFP-positive cells with condensed and fragmented nuclei were counted. Under our experimental conditions, enforced expression of p53 led to an increase in the number of apoptotic cells as compared with the control transfection (Fig. 8*B*). In agreement with the above cell survival assay, co-expression of p53 with FLAG-Plk1 decreased the number of apoptotic cells as compared with that resulting from expression of p53 alone. Taken together, these results indicate that Plk1 is an efficient inhibitor of p53.

Kinase-deficient Plk1 Fails to Inhibit p53—Next, we tested whether the Plk1 kinase activity could be required for Plk1-dependent inhibition of the p53 transcriptional activity. As described previously (22), the mutant form of Plk1 (Plk1-K82M), in which Lys^{82} within the ATP-binding motif is replaced by Met, completely lost the kinase activity. We therefore generated an expression plasmid encoding FLAG-Plk1(K82M), and then examined whether Plk1(K82M) could associate with p53, and also affect the p53-mediated transcriptional activation. Immunoprecipitation followed by Western detection of endogenous p53 indicated that p53 interacted with both the wild-type Plk1 and the kinase-deficient Plk1(K82M) (Fig. 9*A*). The effects of the lysine mutation on the p53-mediated transcriptional activation were tested by luciferase reporter analysis. In contrast to the wild-type Plk1, the kinase-deficient Plk1(K82M) failed to reduce the p53-mediated reporter expression driven by those constructs (Fig. 9, *B–D*).

To examine the effect of Plk1(K82M) on p53-dependent apoptosis, H1299 cells were transfected with the expression plasmid for p53 along with or without the expression plasmid for FLAG-Plk1(K82M). Forty-eight hours after transfection, their viability was measured by cell survival assay. As expected, the p53-dependent decrease in the number of viable cells was unaffected in the presence of the exogenous FLAG-Plk1(K82M) (Fig. 9*E*). Taken together, our results strongly suggest that the kinase activity of Plk1 is required for Plk1-dependent inhibition of p53.

ATM Antagonizes the Inhibitory Effect of Plk1 on p53—Plk1 kinase activity has been shown to be inhibited in an ATM-dependent manner in response to DNA damage (19, 20). The kinase activity of ATM was significantly increased after DNA damage, and ATM was able to phosphorylate p53 at the NH_2 terminus on serine 15 to enhance its stability as well as its transactivation activity (48–50). To examine whether ATM could affect the Plk1-mediated inhibition of p53, we transiently co-transfected H1299 cells with expression plasmids for p53 and FLAG-Plk1 together with or without increasing amounts of ATM expression plasmid, and the ability of p53 to drive transcription from the $p21^{WAF1}$ reporter was measured. As expected, co-expression of p53 with ATM resulted in an increase in the transcriptional activity of p53 as compared with that of cells expressing p53 alone (Fig. 10). Increasing amounts of ATM largely abrogated the Plk1-mediated inhibition of the p53-dependent transcriptional activation. It thus appears that ATM could inhibit the activity of Plk1 and thereby restore the transcriptional activity of p53.

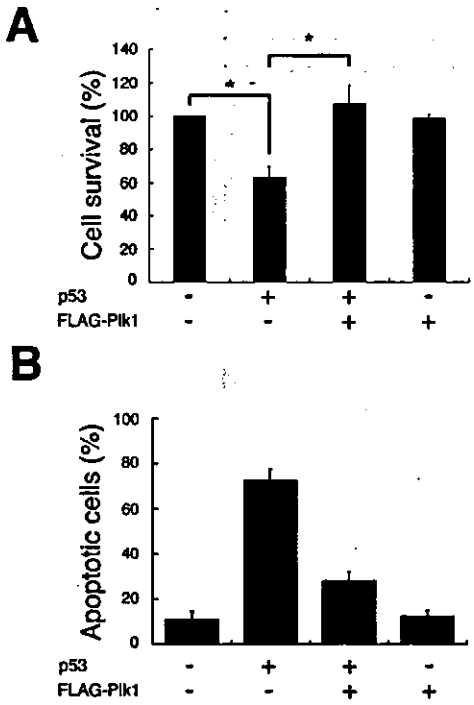

FIG. 8. **Plk1 inhibits the pro-apoptotic activity of p53.** *A*, H1299 cells were transiently co-transfected with 0.6 μg of the expression plasmid for p53 together with or without 1.2 μg of the FLAG-Plk1 expression plasmid. The total amount of plasmid DNA was kept constant (2 μg) with the empty plasmid. At 48 h after transfection, cell viability was determined by MTT cell survival assays. The graph (mean ± S.D. of three independent experiments) represents relative viability based on the percent of viable cells compared with the control transfection (pcDNA3). The percentage of viable cells expressing p53 alone is significantly different from that of viable cells expressing p53 and FLAG-Plk1 ($p < 0.0001$). *B*, H1299 cells were transiently co-transfected with the indicated combinations of the expression plasmids. A constant amount of the GFP expression plasmid (200 ng) was included in all combinations, and the total amount of plasmid DNA was kept constant (2 μg) by including an appropriate amount of empty plasmid. Forty-eight hours after transfection, transfected cells were identified by the presence of green fluorescence. Cell nucleus was stained with propidium iodide to reveal nuclear condensation and fragmentation. The number of GFP-positive cells with condensed and fragmented nuclei was scored, and the percentage of apoptotic cells shown in each column represents the mean of three independent experiments.

DISCUSSION

In the present study, we have found that Plk1 interacts with p53 and inhibits its transactivation as well as apoptosis-inducing activity in mammalian cultured cells. This interaction is mediated by the sequence-specific DNA-binding domain of p53 and the region of Plk1 containing the kinase domain. Importantly, Plk1-mediated inhibition of p53 requires its kinase activity and is attenuated with ATM. Thus, our present data support the hypothesis that p53 is one of the critical targets of Plk1, and that Plk1-mediated inhibition of p53 contributes at least in part to cell fate decisions regarding survival and tumorigenesis.

The expression of *Plk1* was significantly down-regulated in response to cisplatin treatment. Recently, Ree *et al.* (51) found that ionizing radiation leads to the suppression of *Plk1* mRNA expression. It is of interest to examine whether genotoxic stresses other than cisplatin and ionizing radiation could also repress the expression of *Plk1*. On the other hand, *Plk1* mRNA expression is significantly induced in various human primary tumors (27). It is necessary to identify the promoter region as well as the transcription factor(s) required for the transcriptional regulation of *Plk1* in cancerous cells. In good agreement with the previous observations (52), Uchiumi *et al.* (53) have identified the regulatory regions responsible for the activation of the human *Plk1* promoter, which include a consensus Sp1-binding site and a CCAAT box. It has been shown that the transcription factor NF-Y, a heterotrimeric complex consisting of NF-YA, NF-YB, and NF-YC, recognizes and binds to the CCAAT box (54). Indeed, the electrophoretic mobility shift assay revealed that NF-Y binds to the CCAAT box present within the human *Plk1* promoter region, however, it remains to be determined whether NF-Y and/or Sp1 could actually transactivate the *Plk1* promoter in tumor cells (53). Recently, Lee and Pedersen (55) have reported that there exist 6 GC boxes and the CCAAT box within the *type II hexokinase* (*HKII*) promoter, and that NF-Y and Sp family members including Sp1 might contribute to up-regulation of the *HKII* gene in tumor cells. Further studies regarding the transcriptional regulation of the *Plk1* gene are necessary to clarify the molecular mechanisms of Plk1-dependent tumorigenesis.

During the DNA damage response, the activity of ATM is significantly increased and is responsible for the rapid phosphorylation of p53 at Ser^{15} (48–50). This ATM-dependent phosphorylation contributes to the increased stability and activity of p53 by facilitating its dissociation from MDM2 (56). In addition, phosphorylation of p53 at Ser^{15} induces its binding to the transcriptional co-activator p300 (57). Recently, it has been shown that Plk1 activity is inhibited in response to DNA damage, and this inhibition occurs in an ATM-dependent manner (19, 20). Our present data demonstrate that the Plk1-mediated inhibition of p53 activity is rescued by the co-expression of ATM, suggesting that, in addition to the ATM-dependent phosphorylation of p53, the activity of p53 may be enhanced at least in part by the ATM-dependent inhibition of Plk1. Intriguingly, Liu and Erikson (33) reported that p53 is significantly stabilized in Plk1-depleted cells. In accordance with their findings, we have shown that the exposure of SH-SY5Y cells to cisplatin leads to a remarkable accumulation of p53, which is strongly associated with a significant down-regulation of the endogenous Plk1 both at mRNA and protein levels, suggesting that Plk1 is closely involved in the regulation of p53 stability and thereby modulates its activity. Under our experimental conditions, however, overexpression of FLAG-Plk1 did not affect the amounts of the endogenous as well as the ectopically expressed p53.

The pro-apoptotic function of p53 involves its ability to act as a transcription factor in transactivating downstream target gene promoters. The majority of missense mutations of p53 detected in human tumors occur within its sequence-specific DNA-binding domain, and these mutations cause the loss of p53 activity (58). Thus, the structural integrity of this domain is required for p53 function. On the other hand, several viral and cellular proteins inactivate p53 through a variety of different mechanisms (58). MDM2 and Pirh2 promote ubiquitination and degradation of p53 (59–62). Sir2α interacts with p53 and induces its deacetylation (63). In addition, S100B calcium-binding protein prevents the oligomerization of p53 to inhibit its function (64). Based on our systematic immunoprecipitation analysis, Plk1 binds to p53 through the sequence-specific DNA-binding domain of p53. Intriguingly, SV40 large T antigen binds to the sequence-specific DNA-binding domain of p53, and abrogates DNA binding as well as the transactivation function of p53 (65, 66). It is thus likely that, like SV40 large T antigen, Plk1 might mask this domain of p53 by direct binding, and thereby inhibit its sequence-specific transcriptional activity. Further study is required to identify the detailed molecular mechanism.

In sharp contrast to Plk1, Xie *et al.* (26) found that the kinase

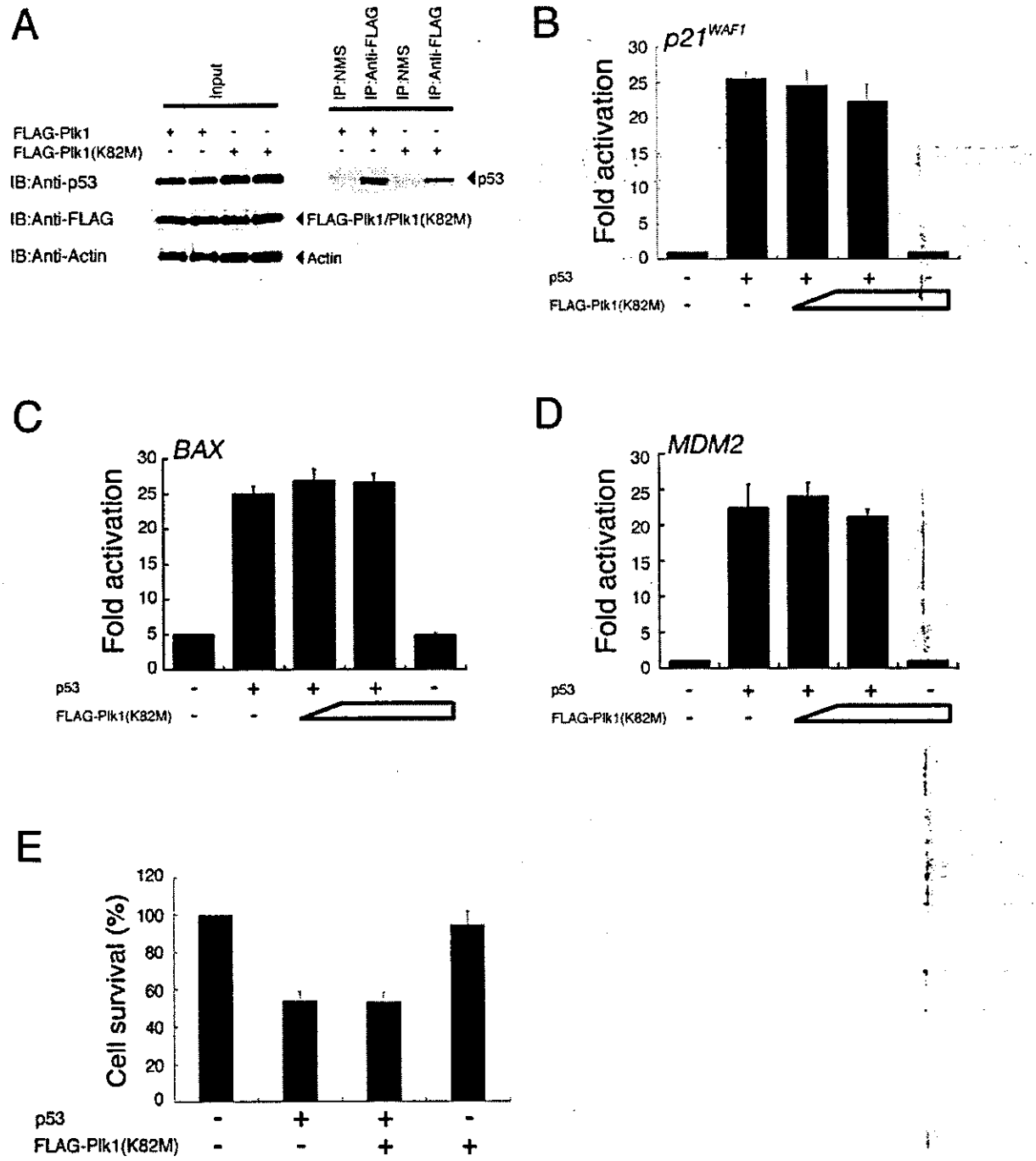

FIG. 9. **Kinase-deficient Plk1(K82M) fails to reduce the activity of p53.** *A*, Plk1(K82M) retains an ability to interact with p53. COS7 cells were transiently transfected with the expression plasmid for FLAG-Plk1 or FLAG-Plk1(K82M). Forty-eight hours after transfection, cell lysates were prepared and subjected to anti-FLAG immunoprecipitation followed by immunoblotting with monoclonal anti-p53 antibody. Immunoprecipitation with NMS was used as a negative control. Equal amounts of protein derived from cell lysates were immunoblotted with monoclonal anti-p53, monoclonal anti-FLAG, or with polyclonal anti-actin antibody. *B–D*, Plk1(K82M) has an undetectable effect on the transcriptional activity of p53. H1299 cells were transiently co-transfected with a fixed amount of the p53 expression plasmid (25 ng) and the p53-responsive luciferase reporter construct carrying the *p21*^{WAF1} (*B*), *BAX* (*C*), or *MDM2* (*D*) promoter (100 ng) in the presence or absence of increasing amounts of the expression plasmid encoding FLAG-Plk1(K82M) (100 or 200 ng). The total amount of plasmid DNA per transfection was kept constant (510 ng) with pcDNA3. Determination and calculation of the luciferase activities are described in the legend to Fig. 6. *E*, Plk1(K82M) is unable to inhibit the pro-apoptotic function of p53. H1299 cells were transiently co-transfected with the p53 expression plasmid (0.6 μg) together with or without the expression plasmid for FLAG-Plk1(K82M) (1.2 μg). Forty-eight hours after transfection, their viability was measured by MTT cell survival assays as described in the legend to Fig. 8.

activity of Plk3 is rapidly enhanced in response to DNA damage in an ATM-dependent fashion. They also described that Plk3 has the ability to interact directly with p53 and phosphorylate p53 at Ser^{20}. Moreover, a kinase-defective mutant form of Plk3 fails to phosphorylate p53, and abrogates the p53-mediated transcriptional activation as well as growth suppression, indicating that Plk3 might enhance the p53 activity through Ser^{20} phosphorylation of p53 (26). In addition to Ser^{15} phosphoryla-

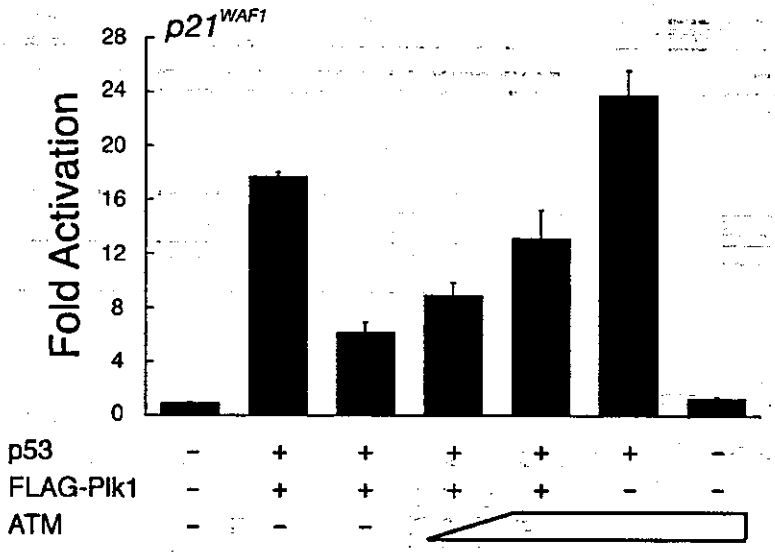

FIG. 10. **ATM antagonizes the inhibitory effect of Plk1 on the p53-dependent transactivation.** H1299 cells were transiently co-transfected with the expression plasmids encoding p53 (25 ng) and FLAG-Plk1 (200 ng) along with the luciferase reporter construct containing the p53-responsive element from the $p21^{WAF1}$ promoter in the presence or absence of increasing amounts of ATM expression plasmid (50 or 100 ng). pcDNA3 was used to equalize the amount of plasmid in each transfection, and the *Renilla* luciferase plasmid was included in the transfection mixture to normalize the transfection efficiency. Determination and calculation of the luciferase activities are described in the legend to Fig. 6.

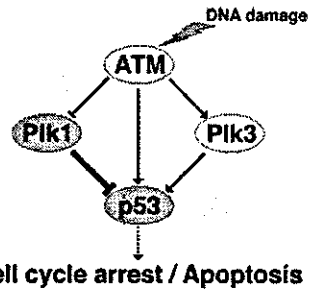

FIG. 11. **Schematic representation of interactions among ATM, Plk1, Plk3, and p53 in response to DNA damage.**

tion of p53, DNA damage-induced phosphorylation of p53 at Ser^{20} prevents its association with MDM2 and results in its stabilization (67). Of note, it has been shown that Plk1 phosphorylates p53 *in vitro* but on residues that might be different from that mediated by Plk3 (26). According to their phosphopeptide mapping analysis, at least three unique radiolabeled tryptic peptides derived from recombinant p53 were detected in the presence of Plk1. Recently, Nakajima *et al.* (68) identified a sequence (D/E)*X*(S/T)ψ*X*(D/E) (*X*, any amino acid; ψ, a hydrophobic amino acid) as a consensus motif for Plk1-dependent phosphorylation (68). During the search for a putative phosphorylation site(s) targeted by Plk1 within the amino acid sequence of p53, we found a related motif (^{254}ITTLED^{259}) present within the sequence-specific DNA-binding domain of p53, suggesting that this motif could be one of the putative phosphorylation sites of p53 targeted by Plk1, although there is no direct evidence for this possibility. According to our present results, the kinase-deficient mutant form of Plk1 that retained an ability to associate with p53, failed to reduce the transcriptional as well as apoptosis-inducing activity of p53, suggesting that the kinase activity of Plk1 is critical for the Plk1-dependent inhibition of p53. Thus, identification of the major phosphorylation site(s) of p53 by Plk1 is required to establish the functional significance of the Plk1-mediated phosphorylation of p53. In contrast, Liu and Erikson (33) reported that, like wild-type mouse Plk1, co-expression of the kinase-defective (K82M) mouse Plk1 partially rescued the apoptotic phenotype induced by the depletion of Plk1, indicating that the kinase activity is not necessary for its anti-apoptotic activity. They also described that their kinase-defective mouse Plk1 has 15–20% of wild-type kinase activity, raising a possibility that the residual kinase activity of their mouse Plk1(K82M) might be enough to inhibit the Plk1 depletion-induced apoptosis.

Fig. 11 shows a model that incorporates our present findings, and illustrates various interactions in response to DNA damage. Given the fact that the differential expression of Plk1 and Plk3 during the cisplatin-induced apoptosis, and their differential effects on p53, it is conceivable that the balance between intracellular expression levels of Plk1 with oncogenic potential and pro-apoptotic Plk3 is at least in part responsible for the determination of the cell fate via the physical and functional interaction with p53.

Acknowledgments—We are grateful to Dr. Y. Shiloh and the Japanese Study Group for Pediatric Liver Tumor for kindly providing the ATM expression plasmid and hepatoblastoma tissues, respectively. We thank Dr. S. Sakiyama and members of our laboratory for helpful discussions. We also thank Y. Nakamura and M. Kikawa for excellent technical assistance.

REFERENCES

1. Glover, D. M., Hagan, I. M., and Tavares, A. A. (1998) *Genes Dev.* **12**, 3777–3787
2. Clay, F. J., McEwen, S. J., Bertoncello, I., Wilks, A. F., and Dunn, A. R. (1993) *Proc. Natl. Acad. Sci. U. S. A.* **90**, 4882–4886
3. Lee, K. S., Grenfell, T. Z., Yarm, F. R., and Erikson, R. L. (1998) *Proc. Natl. Acad. Sci. U. S. A.* **95**, 9301–9306
4. Song, S., Grenfell, T., Garfield, S., Erikson, R. L., and Lee, K. S. (2000) *Mol. Cell. Biol.* **20**, 286–298
5. Jang, Y.-J., Lin, C.-Y., Ma, S., and Erikson, R. L. (2002) *Proc. Natl. Acad. Sci. U. S. A.* **99**, 1984–1989
6. Glover, D. M., Ohkura, H., and Tavares, A. (1996) *J. Cell Biol.* **135**, 1681–1684
7. Lane, H., and Nigg, E. A. (1997) *Trends Cell. Biol.* **7**, 63–68
8. Nigg, E. A. (1998) *Curr. Opin. Cell Biol.* **10**, 776–783
9. Hamanaka, R., Maloid, S., Smith, M. R., O'Connell, C. D., Longo, D. L., and Ferris, D. K. (1994) *Cell Growth & Differ.* **5**, 249–257
10. Smith, M. R., Wilson, M. L., Hamanaka, R., Chase, D., Kung, H.-F., Longo, D. L., and Ferris, D. K. (1997) *Biochem. Biophys. Res. Commun.* **234**, 397–405
11. Lake, R. J., and Jelinek, W. R. (1993) *Mol. Cell. Biol.* **13**, 7793–7801
12. Golsteyn, R. M., Schultz, S. J., Bartek, J., Ziemiecki, A., Ried, T., and Nigg, E. A. (1994) *J. Cell Sci.* **107**, 1509–1517
13. Holtrich, U., Wolf, G., Brauninger, A., Karn, T., Bohme, B., Rubsamen-Waigmann, H., and Strebhardt, K. (1994) *Proc. Natl. Acad. Sci. U. S. A.* **91**, 1736–1740
14. Simmons, D. L., Neel, B. G., Stevens, R., Evett, G., and Erikson, R. L. (1992) *Mol. Cell. Biol.* **12**, 4164–4169
15. Donohue, P. J., Alberts, G. F., Guo, Y., and Winkles, J. A. (1995) *J. Biol. Chem.* **270**, 10351–10357
16. Golsteyn, R. M., Mundt, K. E., Fry, A. M., and Nigg, E. A. (1995) *J. Cell Biol.* **129**, 1617–1628
17. Hamanaka, R., Smith, M. R., O'Connor, P. M., Maloid, S., Mihalic, K., Spivak, J. L., Longo, D. L., and Ferris, D. K. (1995) *J. Biol. Chem.* **270**, 21086–21091
18. Qian, Y.-W., Erikson, E., and Maller, J. L. (1998) *Science* **282**, 1701–1704
19. Smits, V. A., Klompmaker, R., Arnaud, L., Rijksen, G., Nigg, E. A., and Medema, R. H. (2000) *Nat. Cell Biol.* **2**, 672–676
20. van Vugt, M. A. T. M., Smits, V. A. J., Klompmaker, R., and Medema, R. H. (2001) *J. Biol. Chem.* **276**, 41656–41660
21. Toyoshima-Morimoto, F., Taniguchi, E., Shinya, N., Iwamatsu, A., and

Nishida, E. (2001) *Nature* **410**, 215–220
22. Yuan, J., Eckerdt, F., Bereiter-Hahn, J., Kurunci-Csacsko, E., Kaufmann, M., and Strebhardt, K. (2002) *Oncogene* **21**, 8282–8292
23. Toyoshima-Morimoto, F., Taniguchi, E., and Nishida, E. (2002) *EMBO Rep.* **3**, 341–348
24. Ouyang, B., Pan, H., Lu, L., Li, J., Stambrook, P., Li, B., and Dai, W. (1997) *J. Biol. Chem.* **272**, 28646–28651
25. Bahassi, E. M., Conn, C. W., Myer, D. L., Hennigan, R. F., McGowan, C. H., Sanchez, Y., and Stambrook, P. J. (2002) *Oncogene* **21**, 6633–6640
26. Xie, S., Wu, H., Wang, Q., Cogswell, J. P., Husain, I., Conn, C., Stambrook, P., Jhanwar-Uniyal, M., and Dai, W. (2001) *J. Biol. Chem.* **276**, 43305–43312
27. Yuan, J., Horlin, A., Hock, B., Stutte, H. J., Rubsamen-Waigmann, H., and Strebhardt, K. (1997) *Am. J. Pathol.* **150**, 1165–1172
28. Wolf, G., Elez, R., Doermer, A., Holtrich, U., Ackermann, H., Stutte, H. J., Altmannsberger, H. M., Rubsamen-Waigmann, H., and Strebhardt, K. (1997) *Oncogene* **14**, 543–549
29. Knecht, R., Elez, R., Oechler, M., Solbach, C., von Ilberg, C., and Strebhardt, K. (1999) *Cancer Res.* **59**, 2794–2797
30. Knecht, R., Oberhauser, C., and Strebhardt, K. (2000) *Int. J. Cancer* **89**, 535–536
31. Spankuch-Schmitt, B., Wolf, G., Solbach, C., Loibl, S., Knecht, R., Stegmuller, M., von Minckwitz, G., Kaufmann, M., and Strebhardt, K. (2002) *Oncogene* **21**, 3162–3171
32. Spankuch-Schmitt, B., Bereiter-Hahn, J., Kaufmann, M., and Strebhardt, K. (2002) *J. Natl. Cancer Inst.* **94**, 1863–1877
33. Liu, X., and Erikson, R. L. (2003) *Proc. Natl. Acad. Sci. U. S. A.* **100**, 5789–5794
34. Li, B., Ouyang, B., Pan, H., Reissmann, P. T., Slamon, D. J., Arceci, R., Lu, L., and Dai, W. (1996) *J. Biol. Chem.* **271**, 19402–19408
35. Dai, W., Li, Y., Ouyang, B., Pan, H., Reissmann, P., Li, J., Wiest, J., Stambrook, P., Gluckman, J. L., Noffsinger, A., and Bejarano, P. (2000) *Genes Chromosomes Cancer* **27**, 332–336
36. Conn, C. W., Hennigan, R. F., Dai, W., Sanchez, Y., and Stambrook, P. J. (2000) *Cancer Res.* **60**, 6826–6831
37. Xie, S., Wang, Q., Wu, H., Cogswell, J., Lu, L., Jhanwar-Uniyal, M., and Dai, W. (2001) *J. Biol. Chem.* **276**, 36194–36199
38. Nakamura, Y., Ozaki, T., Nakagawara, A., and Sakiyama, S. (1997) *Eur. J. Cancer* **33**, 1986–1990
39. Nakagawa, T., Takahashi, M., Ozaki, T., Watanabe, K., Todo, S., Mizuguchi, H., Hayakawa, T., and Nakagawara, A. (2002) *Mol. Cell. Biol.* **22**, 2575–2585
40. Watanabe, K., Ozaki, T., Nakagawa, T., Miyazaki, K., Takahashi, M., Hosoda, M., Hayashi, S., Todo, S., and Nakagawara, A. (2002) *J. Biol. Chem.* **277**, 15113–15123
41. Kim, E.-J., Park, J.-S., and Um, S.-J. (2002) *J. Biol. Chem.* **277**, 32020–32028
42. Taniguchi, E., Totoshima-Morimoto, F., and Nishida, E. (2002) *J. Biol. Chem.* **277**, 48884–48888
43. Kastan, M. B., Zhan, Q., el-Deiry, W. S., Carrier, F., Jacks, T., Walsh, W. V., Plunkett, B. S., Vogelstein, B., and Fornace, A. J., Jr. (1992) *Cell* **71**, 587–597
44. Shaulsky, G., Goldfinger, N., Ben-Ze'ev, A., and Rotter, V. (1990) *Mol. Cell. Biol.* **10**, 6565–6577
45. Dang, C. V., and Lee, W. M. (1989) *J. Biol. Chem.* **264**, 18019–18023
46. Zaika, A. I., Slade, N., Erster, S. H., Sansome, C., Joseph, T. W., Pearl, M., Chalas, E., and Moll, U. M. (2002) *J. Exp. Med.* **196**, 765–780
47. Zeng, X., Chen, L., Jost, C. A., Maya, R., Keller, D., Wang, X., Kaelin, W. G., Oren, M., Chen, J., and Lu, H. (1999) *Mol. Cell. Biol.* **19**, 3257–3266
48. Banin, S., Moyal, L., Shieh, S., Taya, Y., Anderson, C. W., Chessa, L., Smorodinsky, N. I., Prives, C., Reiss, Y., Shiloh, Y., and Ziv, Y. (1998) *Science* **281**, 1674–1677
49. Canman, C. E., Lim, D. S., Cimprich, K. A., Taya, Y., Tamai, K., Sakaguchi, K., Appella, E., Kastan, M. B., and Siliciano, J. D. (1998) *Science* **281**, 1677–1679
50. Khanna, K. K., Keating, K. E., Kozlov, S., Scott, S., Gatei, M., Hobson, K., Taya, Y., Gabrielli, B., Chan, D., Lees Miller, S. P., and Lavin, M. F. (1998) *Nat. Genet.* **20**, 398–400
51. Ree, A. H., Bratland, A., Nome, R. V., Stokke, T., and Fodstad, O. (2003) *Oncogene* **22**, 8952–8955
52. Brauninger, A., Strebhardt, K., and Rubsamen-Waigmann, H. (1995) *Oncogene* **11**, 1793–1800
53. Uchiumi, T., Longo, D. L., and Ferris, D. K. (1997) *J. Biol. Chem.* **272**, 9166–9174
54. Mantovani, R. (1999) *Gene (Amst.)* **239**, 15–27
55. Lee, M. G., and Pedersen, P. L. (2003) *J. Biol. Chem.* **278**, 41047–41058
56. Shieh, S. Y., Ikeda, M., Taya, Y., and Prives, C. (1997) *Cell* **91**, 325–334
57. Lambert, P. F., Kashanchi, F., Radonovich, M. F., Shiekhattar, R., and Brady, J. N. (1998) *J. Biol. Chem.* **273**, 33048–33053
58. Prives, C., and Hall, P. A. (1999) *J. Pathol.* **187**, 112–126
59. Haupt, Y., Maya, R., Kazaz, A., and Oren, M. (1997) *Nature* **387**, 296–299
60. Kubbutat, M. H. G., Jones, S. N., and Vousden, K. H. (1997) *Nature* **387**, 299–303
61. Honda, R., Tanaka, H., and Yasuda, Y. (1997) *FEBS Lett.* **420**, 25–27
62. Leng, R. P., Lin, Y., Ma, W., Wu, H., Lemmers, B., Chung, S., Parant, J. M., Lozano, G., Hakem, R., and Benchimol, S. (2003) *Cell* **112**, 779–791
63. Luo, J., Nikolaev, A. Y., Imai, S., Chen, D., Su, F., Shiloh, A., Guarente, L., and Gu, W. (2001) *Cell* **107**, 137–148
64. Lin, J., Blake, M., Tang, C., Zimmer, D., Rustandi, R. R., Weber, D. J., and Carrier, F. (2001) *J. Biol. Chem.* **276**, 35037–35041
65. Tan, T.-H., Wallis, J., and Levine, A. J. (1986) *J. Virol.* **59**, 574–583
66. Farmer, G., Bargonetti, J., Zhu, H., Friedman, P., Prywes, R., and Prives, C. (1992) *Nature* **358**, 83–86
67. Vousden, K. H. (2002) *Biochim. Biophys. Acta* **1602**, 47–59
68. Nakajima, H., Toyoshima-Morimoto, F., Taniguchi, E., and Nishida, E. (2003) *J. Biol. Chem.* **278**, 25277–25280

Elevated expression of DNA polymerase κ in human lung cancer is associated with p53 inactivation: Negative regulation of *POLK* promoter activity by p53

YANQING WANG[1,4], MIKA SEIMIYA[1], KIYOKO KAWAMURA[1], LING YU[1], TOMOO OGI[5], KEIZO TAKENAGA[2], TOMOTANE SHISHIKURA[3], AKIRA NAKAGAWARA[3], SHIGERU SAKIYAMA[3], MASATOSHI TAGAWA[1] and JIYANG O-WANG[1]

Divisions of [1]Pathology, [2]Chemotherapy and [3]Biochemistry, Chiba Cancer Center Research Institute, Chiba 260-8717, Japan; [4]Department of Neurobiology, State Key Laboratory of Medical Neurobiology, Medical Center of Fudan University, Shanghai 200032, P.R. China; [5]Institute of Virus Research, Kyoto University, Kyoto 606-8507, Japan

Received December 21, 2003; Accepted February 25, 2004

Abstract. DNA polymerase κ (POLκ) is a low fidelity translesional DNA polymerase implicated in spontaneous and DNA damage-induced mutagenesis. We have previously shown that POLκ was frequently overexpressed in human lung cancer tissues as compared with their matched non-tumorous tissue counterpart. In the present study, we found a close correlation between elevated POLκ expression and p53 inactivation in lung cancer tissues. To investigate whether *POLK* expression might be regulated by p53, we have determined the transcriptional initiation site of *POLK* gene and examined its promoter activity in A549, H358-129, and PC-3 human lung cancer cell lines. Wild-type p53, but not a mutant p53 (R273H) devoid of the DNA-binding activity, strongly inhibited *POLK* promoter activity in these cells. In addition, *POLK* promoter exhibited a significantly higher activity in $p53^{-/-}$ murine embryo fibroblasts (MEF) than in $p53^{+/-}$ and $p53^{+/+}$ MEF. These results link p53 status with POLκ expression and suggest that loss of p53 function may in part contribute to the observed POLκ upregulation in human lung cancers.

Introduction

A growing number of specialized DNA polymerases (Pols) have been identified in the past few years (1-3). These Pols exhibit relaxed fidelity during DNA synthesis and are capable of replicating DNA past unrepaired lesions. DNA polymerase κ (POLκ) is a member of the newly defined Pol Y family (4). Biochemical analyses indicate that POLκ can accurately and efficiently bypass DNA adducts induced by benzo(a)-pyrene (BaP) (5,6), a major carcinogen contained in tobacco smoke. Consistently, studies using Polκ-deficient embryonic stem cells revealed an essential role for Polκ in protecting mammalian cells from BaP-induced lethal and mutagenic effects (7). On the other hand, POLκ has been shown to erroneously bypass some other DNA lesions, including N-2-acetylaminofluorene guanine adduct and 8-oxoguanine (8-11). In addition, POLκ is also highly mutagenic when replicating undamaged DNA (9,12) and its transient overexpression in murine fibroblasts causes a 10-fold increase in the mutation frequency of endogenous *Hprt* locus (13). These results suggest that while POLκ functions to suppress BaP-induced mutagenesis, it may simultaneously enhance spontaneous mutations as well as mutations induced by other DNA damaging agents.

The opposing effects of POLκ in BaP-induced vs spontaneous mutagenesis suggest that its expression must be strictly regulated. POLκ is expressed at low levels in most normal tissues except for the testis, adrenal gland and ovary, where it may be required for the bypass of physiologically arising base damage (13-15). Interestingly, *POLK* promoter contains a consensus motif for the arylhydrocarbon receptor (AhR), a ligand-activated transcription factor with high affinities for aromatic compounds such as BaP and 3-methylcholanthrene (3MC). Indeed, *POLK* expression is inducible by 3MC in an AhR-dependent manner (16), consistent with its role in the error-free bypass of DNA adducts induced by these aromatic compounds (5,6).

We previously found that POLκ was frequently overexpressed in human lung cancer tissues as compared with their matched non-tumorous tissues (17). The elevated POLκ expression was not due to *POLK* gene amplification or its translocation to the vicinity of an actively transcribed gene (17). Moreover, no point mutations were found in the *POLK* promoter region isolated from a lung cancer tissue that overexpressed POLκ (unpublished results). These results suggest

Correspondence to: Dr Jiyang O-Wang, Laboratory for B Lymphocyte Function, Research Center for Allergy and Immunology, 666-2 Nitona, Chuo-ku, Chiba 260-8717, Japan
E-mail: oh@chiba-ccri.chuo.chiba.jp

Key words: DNA polymerase κ, p53, transcription, lung cancer

that the observed POLκ upregulation in tumor is likely due to dysregulated transcription.

In the present study, we have focused on p53, a transcription factor and a tumor suppressor that is inactivated in over 50% of human cancers (18). We initially examined p53 status in representative lung cancer tissues expressing different levels of POLκ and found a good correlation between elevated POLκ expression and p53 inactivation. Further analysis revealed that human *POLK* promoter activity was negatively regulated by p53.

Materials and methods

Tissue specimens. Surgically resected tumors and their adjacent normal tissue (>3 cm away from the tumor) were obtained from the Chiba Cancer Center Tissue Bank as frozen tissues. Loss of heterozygosity (LOH) of the p53 allele as well as the yeast functional assay for p53 activity was performed as described previously (19,20).

Cell culture. Mouse embryonic fibroblasts (MEF) were established from E13.5 embryos derived from crossing $p53^{+/-}$ mice, and genotyped as described previously (21). MEF and A549 cells were maintained in DMEM supplemented with 10% FCS and 50 units of penicillin-streptomycin. H358-129 and PC-3 human lung cancer cells were cultured in RPMI medium containing 10% FCS.

Determination of POLK transcriptional initiation site. Total RNA was extracted from human lung cancer tissues of two patients. RNA ligase mediated rapid amplification of cDNA ends (RLM-RACE) was carried out using an RLM-RACE kit (Amibion, Austin, TX) according to the company's protocol. The PCR products derived from Tobacco Acid Pyrophosphatase (TAP)-treated RNA were subcloned in pCR2.1 (Invitrogen Corp., Carlsbad, CA) and sequenced to determine the 5' end of *POLK* mRNA.

Plasmid constructs. A 730-bp *POLK* promoter fragment (corresponding to nucleotides -725 to +5 relative to the transcriptional start site) was cloned into PGL2 (Promega, Madison, WI) to generate the luciferase reporter vector POLK-luc. The human wild type p53 expression vector p5C53-wt was a kind gift from Dr B. Vogelstein. The mutant p53 cDNA (p53-R273H) was cloned from a colon cancer cell line (HT-29). The enhanced green fluorescence protein expression vector pEGFP was purchased from Clontech (Palo Alto, CA).

Transient transfection and the dual luciferase reporter assay. Cells were seeded in 6-well plates and allowed to grow until they were 40-50 confluent. POLK-luc vector (2 μg) was cotransfected with the same amount of p5C53-wt, p53-R273H or control pCDNA3.1/lacZ vector using Lipofectin reagent (Invitrogen Corp.) according to the recommended protocol. The renilla luciferase expression vector (0.4 μg), driven by herpes simplex virus-thymidine kinase promoter (pRL-TK, Promega), was included as an internal standard of transfection efficiency. Luciferase assay was performed as previously described (22). The luciferase activity was calculated as the percentage of the activity of renilla luciferase. Each experiment was repeated three times and a typical result is shown.

Table I. Correlation of elevated POLκ expression with p53 inactivation in human lung cancer tissues.

Case	POLκ expression level[a]	LOH[b]	% red colony[c]	p53 status[d]
98-635	-		9	WT
96-49	-		11	WT
96-45	-	LOH	12	WT
96-54	+	LOH	56	Mutant
98-668	++	LOH	24	Mutant
98-616	+		48	Mutant

[a]-, low; +, medium; ++, high (17). [b]Loss of heterozygosity of the p53 loci as determined by allelic-specific PCR (20). [c]Determined dy the yeast functional assay (19). [d]p53 status was judged based on the results of both LOH and the percentage of red colony, assuming a maximum of 50% normal tissue contamination.

Cell cycle analysis. A549 cells were transfected with pEGFP (2 μg) in the presence of 2 μg of either p5C53-wt or pCDNA3.1/lacZ. Two days later, cells were collected and incubated in 200 μl PBS containing 0.1% RNase A, 0.1% Triton at room temprerature for 10 min, followed by staining in PBS containing 50 μg/ml of propidium iodide on ice for 30 min. EGFP expression and DNA contents were analyzed with a FACScan flow cytometer (Becton-Dickinson, Mountain View, CA).

Results

Correlation of elevated POLK expression with p53 inactivation in human lung cancer tissues. We first examined p53 status in representative lung cancer tissues with different levels of POLκ expression. LOH analysis indicated that 3 of 6 cases examined had only one intact p53 allele (Table I). To determine the p53 activity, we next utilized a yeast functional assay in which a mutant p53 gene can be identified as a red colony (19). The percentage of the red colony, combined with the result of LOH, indicated that p53 was inactivated in three cases. As shown in Table I, there was a close inverse correlation between elevated POLκ expression and p53 inactivation.

Determination of POLK transcriptional initiation site. To directly investigate a potential role for p53 in the regulation of *POLK* gene expression, we determined the *POLK* transcriptional initiation site in a human lung cancer tissue by using an RLM-RACE method. We obtained a major PCR product of 471-bp and a minor product of 324-bp (Fig. 1A). Sequence analysis revealed that both products have the same 5'-end and thus represent transcripts from the same transcriptional start site. The minor product, however, lacked exon 2 and was probably derived from alternative splicing (Fig. 1B).

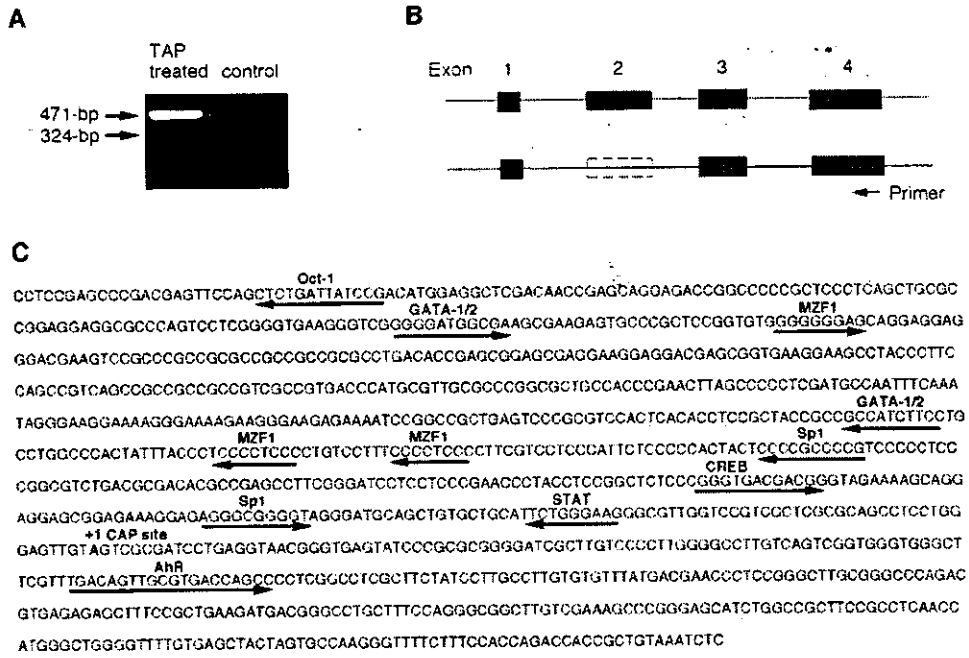

Figure 1. Determination of the transcriptional initiation site of *POLK* gene in human lung cancer tissues. A, PCR amplification of cDNAs derived from TAP-treated or non-treated (control) mRNA. Arrows indicate specific PCR products detected only in TAP-treated sample. B, Schematic illustration of the RLM-RACE products. The 471-bp product contained exons 1 through 4 whereas the 324-bp product lacked exon 2. An arrow indicates the position of the outer primer used in the RLM-RACE. C, *POLK* promoter sequence. Arrows indicate potential DNA-binding motifs for transcription factors. The transcriptional initiation site (CAP site) is shown in bold (+1).

Similar results were obtained with a different lung cancer tissue (data not shown). The transcriptional initiation site determined in the present study is identical with that recently found in the human testis (16). The *POLK* promoter sequence, along with the potential DNA-binding motifs for transcription factors, is shown in Fig. 1C. No apparent p53-binding consensus motif (RRRCWWGYYY) was present in this 1059-bp sequence.

Effects of p53 on POLK promoter activity in human lung cancer cells. We then constructed a luciferase reporter vector driven by the human *POLK* promoter and examined its activity in several human lung cancer cell lines. The luciferase activity was dramatically repressed by co-transfection of wild-type p53 (Fig. 2A) and in a dose-dependent manner (Fig. 2B). Co-transfection of a mutant p53 (R273H) that lacked the DNA-binding activity only had a mild inhibitory effect (Fig. 2C), suggesting that efficient inhibition of *POLK* promoter activity required a functional DNA binding domain of p53.

p53-mediated inhibition of POLK promoter activity was not accompanied by apoptosis induction. Since p53 is known to induce apoptosis as well as cell cycle arrest, the observed decrease of *POLK* promoter activity might be a secondary effect associated with decreased cell viability. To address this point, we examined the effects of transient expression of p53 on cell cycle progression. A549 cells were transfected with p53 or lacZ expression vector in the presence of pEGFP and the cell cycle distribution of the EGFP positive cells was analyzed 48 h later. As shown in Fig. 3, there was no striking difference in the percentages of cells at subG1 (apoptotic), G1 and G2/M phases between cells transfected with p53 and lacZ gene. These

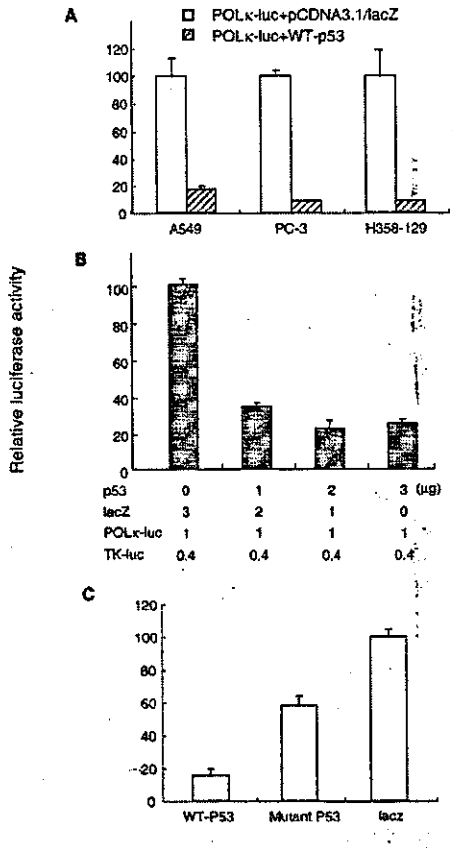

Figure 2. Repression of *POLK* promoter activity by exogenous p53 expression in human lung cancer cell lines. A, POLK-luc was co-transfected with p5C53-wt into A549, H358-129 or PC-3 cells. B, A549 cells were transfected with different amount of p5C53-wt as indicated. C, A549 cells were transfected with p5C53-wt, p53-R273H, or lacZ expression vector. The activity of POLK-luc cotransfected with pCDNA3.1/lacZ was set as 100.

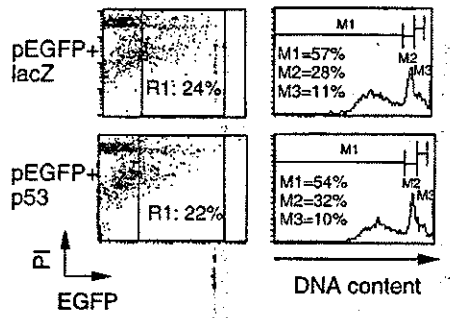

Figure 3. Effects of transient p53 expression on cell cycle progression. A549 cells were transfected with pcDNA3.1/lacZ or p5C53-wt in the presence of pEGFP. Two days later, EGPP positive cells were gated and their DNA contents were analyzed. The percentages of cells at subG1 (M1), G1 (M2) and G2M (M3) are shown.

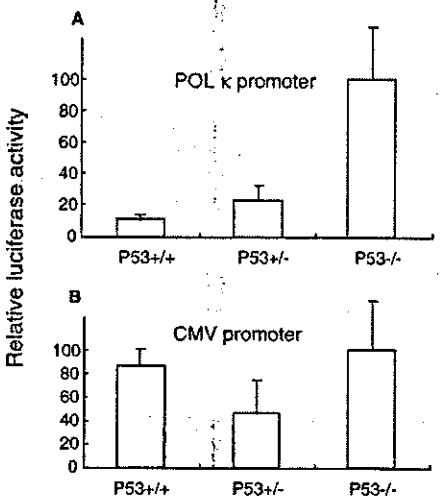

Figure 4. Effects of endogenous p53 on *POLK* promoter activity. POLK-luc or control CMV-luc vector was transfected into $p53^{+/+}$, $p53^{+/-}$ or $p53^{-/-}$ MEF cells and the luciferase activity was examined. In both cases, luciferase activity in $p53^{-/-}$ cells was set at 100.

results indicated that, at least in this transient transfection system, p53 did not induce a significant increase of apoptotic cells.

Effects of endogenous p53 on POLK promoter activity. To further analyze the effects of p53 on *POLK* promoter activity, we next performed *POLK* reporter assay in mouse embryo fibroblasts (MEF) with different p53 status. Consistent with the results obtained with lung cancer cell lines, *POLK* promoter activity was low in $p53^{+/+}$ MEF, slightly increased in $p53^{+/-}$ MEF and significantly elevated in $p53^{-/-}$ MEF cells (Fig. 4A). In contrast to the *POLK* promoter, the CMV promoter exhibited similar activity in MEF cells regardless of their p53 status (Fig. 4B). These results are consistent with a role for p53 in negatively regulating *POLK* promoter activity.

Discussion

Although only a limited number of human lung cancer tissues were examined in the present study, the elevated POLκ expression was found to be correlated with p53 inactivation. Consistent with this observation, human *POLK* promoter exhibited a significantly higher activity in $p53^{-/-}$ cells than in $p53^{+/-}$ and $p53^{+/+}$ cells. These results collectively suggest that loss of p53 function may lead to elevated POLκ transciption.

p53 is a sequence-specific DNA binding protein (23-25) and activates transcription of a variety of genes, including those involved in cell cycle arrest, apoptosis, and DNA repair. In many cases, p53 directly binds to the consensus motif in the promoter or other regulatory region of the target gene to activate the transcription. p53 has also been shown to repress transcription of a number of genes. The mechanism for p53-mediated repression is less clear since many of the p53-repressed genes do not contain a p53-responsive consensus element (26). It has been shown that p53 represses transcription through interations with the basal transcription factors such as TATA-binding protein, or through binding to and interfering with the function of upstream transcriptional activators.

The *POLK* promoter examined in the present study does not contain a TATA box and no p53 consensus motif is present in this region. It is unlikely that p53 directly binds to the human *POLK* promoter region and regulates its expression. In fact, Velasco-Miguel *et al* recently reported that human *POLK* gene was not a direct target of p53 (15). Interestingly, their data also indicated that the basal level of human *POLK* transcripts was significantly higher in p53-null RKO cells than in p53-intact cells (15). These observations, along with the data presented here, suggest that p53 may indirectly suppress *POLK* expression in certain cell types.

The tumor suppressor p53 is a key regulator of cell cycle checkpoint, DNA repair and apoptosis. In response to DNA damage, p53 induces the expression of genes involved in DNA repair and trigger cell cycle arrest to allow sufficient time for repair. p53 thus functions to prevent the accumulation of DNA damage and maintain the genome integrity. Our results link p53 status with *POLK* expression and suggest that p53 may be involved in the regulation of expression of the lesion-bypassing DNA polymerases.

Acknowledgements

This work was supported by a Grant-in-Aid for scientific research on priority areas from the Ministry of Education, Culture, Sports, Science and Technology in Japan.

References

1. Woodgate R: A plethora of lesion-replicating DNA polymerases. Genes Dev 13: 2191-2195, 1999.
2. Friedberg EC, Feaver WJ and Gerlach VL: The many faces of DNA polymerases: strategies for mutagenesis and for mutational avoidance. Proc Natl Acad Sci USA 97: 5681-5683, 2000.
3. Lehmann AR: Replication of UV-damaged DNA: new insights into links between DNA polymerases, mutagenesis and human diseases. Gene 253: 1-12, 2000.
4. Ohmori H, Friedberg EC, Fuchs RP, Goodman MF, Hanaoka F, Hinkel D, Kunkel TA, Lawrence CW, Livneh Z, Nohmi T, Prakash L, Prakash S, Todo T, Walker GC, Wang Z and Woodgate R: The Y-family of DNA polymerases. Mol Cell 8: 7-8, 2001.
5. Zhang Y, Yuan F, Wu X, Wang M, Rechkoblit O, Taylor J-S, Geacintov NE and Wang Z: Error-free and error-prone lesion bypass by human DNA polymerase κ *in vitro*. Nucleic Acids Res 28: 4138-4146, 2000.

6. Suzuki N, Ohashi E, Kolbanovskiy A, Geacintov NE, Grollman AP, Ohmori H and Shibutani S: Translesion synthesis by human DNA polymerase kappa on a DNA template containing a single stereoisomer of dG-(+)- or dG-(-)-anti-N(2)-BPDE (7,8-dihydroxy-anti-9,10-epoxy-7,8,9,10-tetrahydrobenzo(a)pyrene). Biochemistry 41: 6100-6106, 2002.
7. Ogi T, Shinkai Y, Tanaka K and Ohmori H: Polκ protects mammalian cells against the lethal and mutagenic affects of benzo(a)pyrene. Proc Natl Acad Sci USA 99: 15548-15553, 2002.
8. Ohashi E, Ogi T, Kusumoto R, Iwai S, Masutani C, Hanaoka F and Ohmori H: Error-prone bypass of certain DNA lesions by the human DNA polymerase κ. Genes Dev 14: 1589-1594, 2000.
9. Zhang Y, Yuan F, Xin H, Wu X, Rajpal DK, Yang D and Wang Z: Human DNA polymerase κ synthesizes DNA with extraordinarily low fiselity. Nucleic Acids Res 28: 4147-4156, 2000.
10. Gerlach VL, Feaver WJ, Fischhaber PL and Friedberg EC: Purification and characterization of polκ, a DNA polymerase encoded by the human *DINB1* gene. J Biol Chem 276: 92-98, 2001.
11. Suzuki N, Ohashi E, Hayashi K, Ohmori H, Grollman AP and Shibutani S: Translesional synthesis past acetylaminofluorene-derived DNA adducts catalyzed by human DNA polymerase kappa and Escherichia coli DNA Polymerase IV. Biochemistry 40: 15176-15183, 2001.
12. Ohashi E, Bebenek K, Matsuda T, Feaver WJ, Gerlach VL, Friedberg EC, Ohmori H and Kunkel TK: Fidelity and processivity of DNA synthesis by DNA polymerase κ, the product of the human *DINB1* gene. J Biol Chem 275: 39678-39684, 2000.
13. Ogi T, Kato T, Kato T Jr and Ohmori H: Mutation enhancement by DINB1, a mammalian homologue of the Escherichia coli mutagenesis protein dinB. Genes Cells 4: 607-618, 1999.
14. Gerlach VL, Aravind L, Gotway G, Schultz RA, Koonin EV and Friedberg EC: Human and mouse homologs of *Escherichia coli* DinB (DNA Polymerase IV), members of the UmuC/DinB superfamily. Proc Natl Acad Sci USA 96: 11922-11927, 1999.
15. Velasco-Miguel S, Richardson JA, Gerlach VL, Lai WC, Gao T, Russell LD, Hladik CL, White CL III and Friedberg EC: Constitutive and regulated expression of the mouse *Dinb* (Polκ) gene encoding DNA polymerase kappa. DNA Repair 2: 91-106, 2003.
16. Ogi T, Mimura J, Hikida M, Fujimoto H, Fujii-Kuriyama Y and Ohmori H: Expression of human and mouse genes encoding polκ: testis-specific developmental regulation and AhR-dependent inducible transcription. Genes Cells 6: 943-953, 2001.
17. O-Wang J, Kawamura K, Tada Y, Ohmori H, Hideki K, Sakiyama S and Tagawa M: DNA polymerase κ, implicated in spontaneous and DNA damage-induced mutagenesis, is over-expressed in lung cancer. Cancer Res 61: 5366-5369, 2001.
18. Hollstein M, Sidransky D, Vogelstein B and Harris CC: P53 mutations in human cancers. Science 253: 49-53, 1991.
19. Takahashi M, Tonoki H, Tada M, Kashiwazaki H, Furuuchi K, Hamada J, Fujioka Y, Sato Y, Takahashi H, Todo S, Sakuragi N and Moriuchi T: Distinct prognostic values of p53 mutations and loss of estrogen receptor and their cumulative effect in primary breast cancers. Int J Cancer 89: 92-99, 2000.
20. Goto LA, Kanda H, Ishikawa Y, Matsumoto S, Kawaguchi N, Machinami R, Kato Y and Kitagawa T: Association of loss of heterozygosity at the p53 locus with chemoresistance in osteosarcomas. Jpn J Cancer Res 89: 539-547, 1998.
21. Tsukada T, Tomooka Y, Takai S, Ueda Y, Nishikawa S, Yagi T, Tokunaga T, Takeda N, Suda Y, Abe S, Matsuo I, Ikawa Y and Aizawa S: Enhanced proliferative potential in culture of cells from p53-deficient mice. Oncogene 8: 3313-3322, 1993.
22. Maeda T, O-Wang J, Matsubara H, Asano T, Ochiai T, Sakiyama S and Tagawa M: A minimum c-erbB-2 promoter-mediated expression of herpes simplex virus thymidine kinase gene confers selective cytotoxicity of human breast cancer cells to ganciclovir. Cancer Gene Ther 8: 890-896, 2001.
23. Bargonetti J and Manfredi JJ: Multiple roles of the tumor suppressor p53. Curr Opin Oncol 14: 86-91, 2002.
24. Wang L, Wu Q, Qiu P, Mirza A, McGuirk M, Kirschmeier P, Greene JR, Wang Y, Pickett CB and Liu S: Analyses of p53 target genes in the human genome by bioinformatic and microarray approaches. J Biol Chem 276: 43604-43610, 2001.
25. El-Deiry WS, Kern SE, Pietenpol JA, Kinzler KW and Vogelstein B: Definition of a consensus binding site for p53. Nat Genet 1: 45-49, 1992.
26. Ho J and Benchimol S: Transcriptional repression mediated by the p53 tumour suppressor. Cell Death Differ 10: 404-408, 2003.

ELSEVIER

MCN Molecular and Cellular Neuroscience

www.elsevier.com/locate/ymcne
Mol. Cell. Neurosci. 25 (2004) 504–514

Reduced inflammatory pain in mice deficient in the differential screening-selected gene aberrative in neuroblastoma

S. Ohtori,[a,1] E. Isogai,[b,1] F. Hasue,[a] T. Ozaki,[b] Y. Nakamura,[b] A. Nakagawara,[b] H. Koseki,[c] S. Yuasa,[d] E. Hanaoka,[a] J. Shinbo,[a] T. Yamamoto,[e] H. Chiba,[f] M. Yamazaki,[a] H. Moriya,[a] and S. Sakiyama[b,*]

[a] *Department of Orthopaedic Surgery, Graduate School of Medicine, Chiba University, Chuo, Chiba 260-8677, Japan*
[b] *Division of Biochemistry, Chiba Cancer Center Research Institute, Chuo, Chiba 260-8717, Japan*
[c] *Department of Molecular Embryology, Graduate School of Medicine, Chiba University, Chuo, Chiba 260-8677, Japan*
[d] *National Institute of Neuroscience, Kodaira, Tokyo 187-8502, Japan*
[e] *Department of Anaesthesiology, Graduate School of Medicine, Chiba University, Chuo, Chiba 260-8677, Japan*
[f] *Third Department of Anatomy, Graduate School of Medicine, Chiba University, Chuo, Chiba 260-8677, Japan*

Received 10 February 2003; revised 21 November 2003; accepted 1 December 2003

Differential screening-selected gene aberrative in neuroblastoma (Dan) protein is produced in small neurons of dorsal root ganglia. Thermal and mechanical allodynia and Fos expression in the spinal dorsal horn evoked by inflammation and neuropathic pain were investigated using Dan-deficient mice. Mice showed pain reactions induced by the introduction of complete Freund's adjuvant (CFA) into their hind paw (inflammatory pain model) and after sciatic nerve ligation (neuropathic pain model). In the inflammatory pain model, thermal and mechanical pain thresholds in Dan-deficient mice were significantly higher than those of wild-type mice. The number of Fos-immunoreactive cells in the dorsal horn during the inflammatory period was significantly less in Dan-deficient mice. However, in the neuropathic pain model, no differences in thermal hypersensitivity, mechanical allodynia, or the number of Fos-immunoreactive cells in the dorsal horn were observed between the mice. These data suggest that Dan may be a neuromodulator in inflammatory pain.

Introduction

The differential screening-selected gene aberrative in neuroblastoma (*Dan*) was initially cloned as an mRNA down-regulated in v-*src*-transformed rat fibroblasts (Ozaki and Sakiyama, 1993). The analysis of *Dan* function by transfection of cultured cells revealed that *Dan* has an ability to suppress the transformed phenotype and delay entry into the S phase, suggesting that *Dan* carries a tumor-suppressive activity (Ozaki and Sakiyama, 1994; Ozaki et al., 1995). Recently, it has been shown that *Dan* is a founding member of a novel gene family that includes the *Xenopus* head-inducing factor, *Cerberus* and the dorsalizing factor, *Gremlin* (Hsu et al., 1998). *Dan* family members play crucial roles in early mouse embryonic development by inhibiting the signaling derived from bone morphogenetic proteins (BMPs) as well as modulating the action of transforming growth factor β (TGF-β) superfamily members (Hsu et al., 1998; Pearce et al., 1999; Piccolo et al., 1999; Stanley et al., 1998). Dionne et al. (2001) showed that Dan-deficient mice displayed subtle and background-dependent defects, suggesting that functional redundancy exists among *Dan* family members.

We previously showed the existence of Dan in primary small-diameter sensory nerve fibers, and also demonstrated that Dan mediates inflammatory pain, but not pain due to nerve injury (Ohtori et al., 2002). However, the precise mechanism underlying this action is unknown. In the present study, we have produced Dan-deficient mice and investigated inflammation and nerve injury-evoked thermal and mechanical allodynia and Fos expression in the spinal dorsal horn of Dan-deficient and wild-type mice.

Results and discussion

Generation of Dan-deficient mice

Mice with disrupted *Dan* alleles were generated using homologous recombination in embryonic stem cells to replace exons II and III with a neomycin-resistant gene (Fig. 1A). Genotyping of mutant mice was performed by Southern blot (Fig. 1B) and PCR (Fig. 1C) analyses using the probes and primers, respectively, as indicated in Fig. 1A. *Dan* mRNA was expressed in several organs in wild-type mice; however, as expected, it was not detected in Dan-deficient mice (Fig. 1D). Dionne et al. (2001) reported that Dan-deficient mice do not show apparent defects. In the current study, Dan-deficient mice did not show obvious differences when compared with wild-type mice during development, infancy, and adulthood. In the central and peripheral nervous systems, there were no morphologic changes in the Dan-deficient mice.

* Corresponding author. Division of Biochemistry, Chiba Cancer Center Research Institute, 666-2 Nitona, Chuo, Chiba 260-8717, Japan. Fax: +81-43-265-4459.
E-mail address: ssakiyam@chiba-cc.pref.chiba.jp (S. Sakiyama).
[1] These authors have contributed equally to this work.
Available online on ScienceDirect (www.sciencedirect.com.)

1044-7431/$ - see front matter © 2004 Elsevier Inc. All rights reserved.
doi:10.1016/j.mcn.2003.12.002

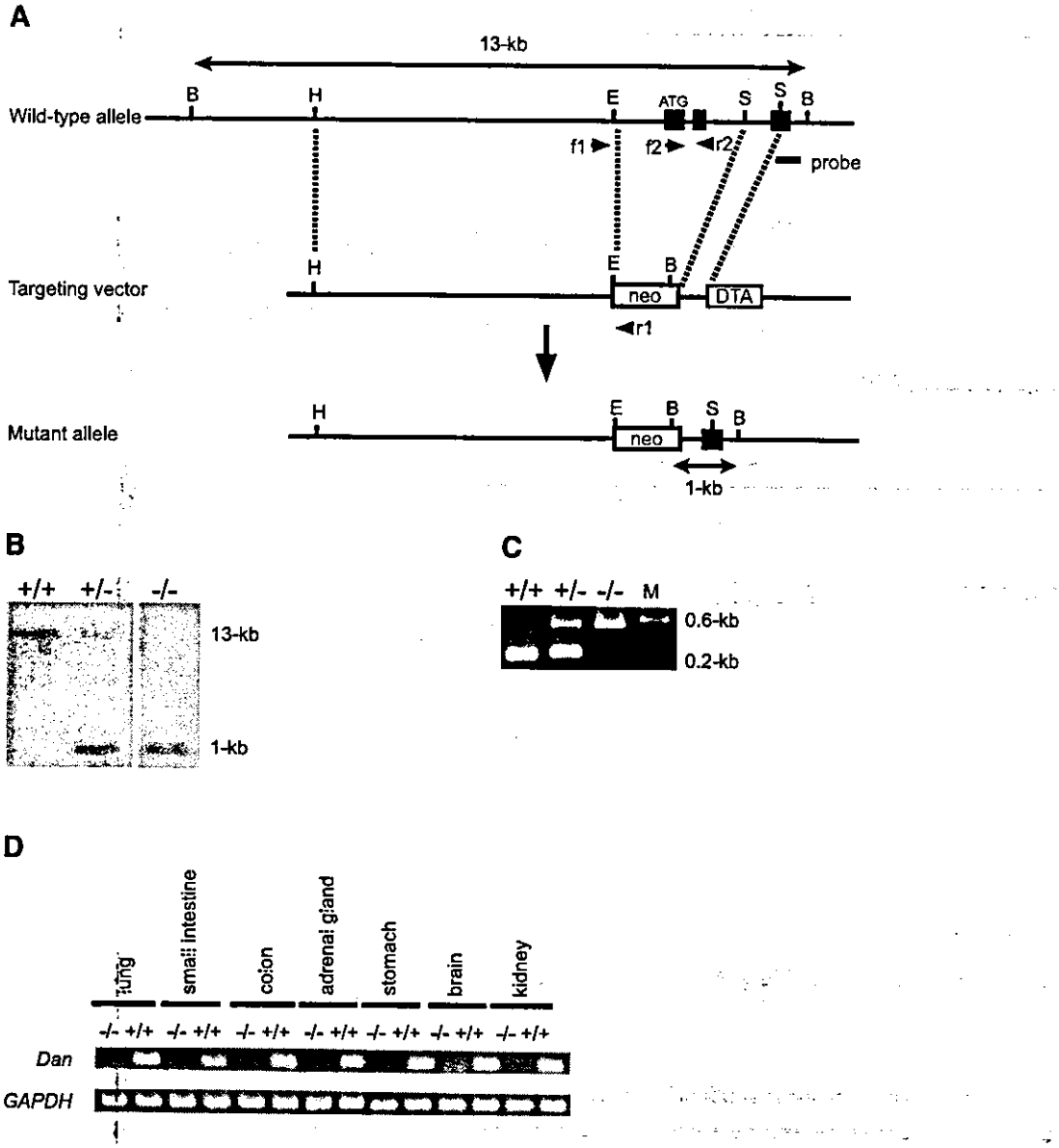

Fig. 1. Generation of Dan-deficient mice. (A) Schematic drawing of gene targeting strategy. The map of the wild-type *Dan* allele spans the region between intron I and exon IV (top). Filled boxes indicate the exons II, III, and IV. The targeting vector (middle) was constructed as described in the Experimental methods. Arrowheads indicate the locations of PCR primers used for detecting the wild-type or mutant allele: forward-1 (f1) and reverse-1 (r1) for the mutant allele, and forward-2 (f2) and reverse-2 (r2) for the wild-type allele. The location of the probe (0.4-kb *SmaI–XbaI* restriction fragment) used for Southern analysis is indicated by the solid bar. This probe detects 13- and 1-kb fragments derived from the wild-type and the mutant alleles, respectively. The mutant allele is shown below the targeting vector. B, *Bam*HI; H, *Hin*cII; E, *Eco*RI; S, *Sma*I. (B) Southern blot analysis of tail DNA from wild-type (+/+), heterozygous (+/−), and homozygous (−/−) mutant mice. Genomic DNA was digested with *Bam*HI, transferred to a nylon membrane, and hybridized with the external probe shown in A. The positions of migration of the fragments derived from wild-type (13 kb) and disrupted alleles (1 kb) are indicated. (C) PCR analysis of tail DNA from wild-type (+/+), heterozygous (+/−), and homozygous (−/−) mutant mice. PCR products were separated on a 2% agarose gel by electrophoresis and visualized by ethidium bromide staining. The positions of migration of the fragments derived from wild-type (0.2 kb) and disrupted alleles (0.6 kb) are indicated. M, DNA molecular weight marker. (D) RT-PCR analysis of *Dan* expression in wild-type (+/+) and homozygous (−/−) mutant mice. Total RNA was prepared from the indicated adult mouse organs and subjected to RT-PCR using specific primers for *Dan* or *GAPDH*. Amplification of *GAPDH* was used as an internal control.

SP, CGRP, NK1, and Dan in the primary sensory neurons under physiological conditions

Double-staining for Dan with CGRP, IB4, P2X3, or NF200

SP- and CGRP-IR neurons were observed in the DRG of both wild-type and Dan-deficient mice (Fig. 2). These neurons were small to intermediate in size. We found that 69 ± 7% (mean ± SE) of all DRG neurons were Dan-IR in wild-type mice, whereas none of DRG neurons were Dan-IR in Dan-deficient mice ($P < 0.01$). The distributions and percentages of SP- and CGRP-IR DRG neurons were not significantly different between wild-type and Dan-deficient mice (wild-type, SP: 26 ± 4%, CGRP, 38 ± 6%;

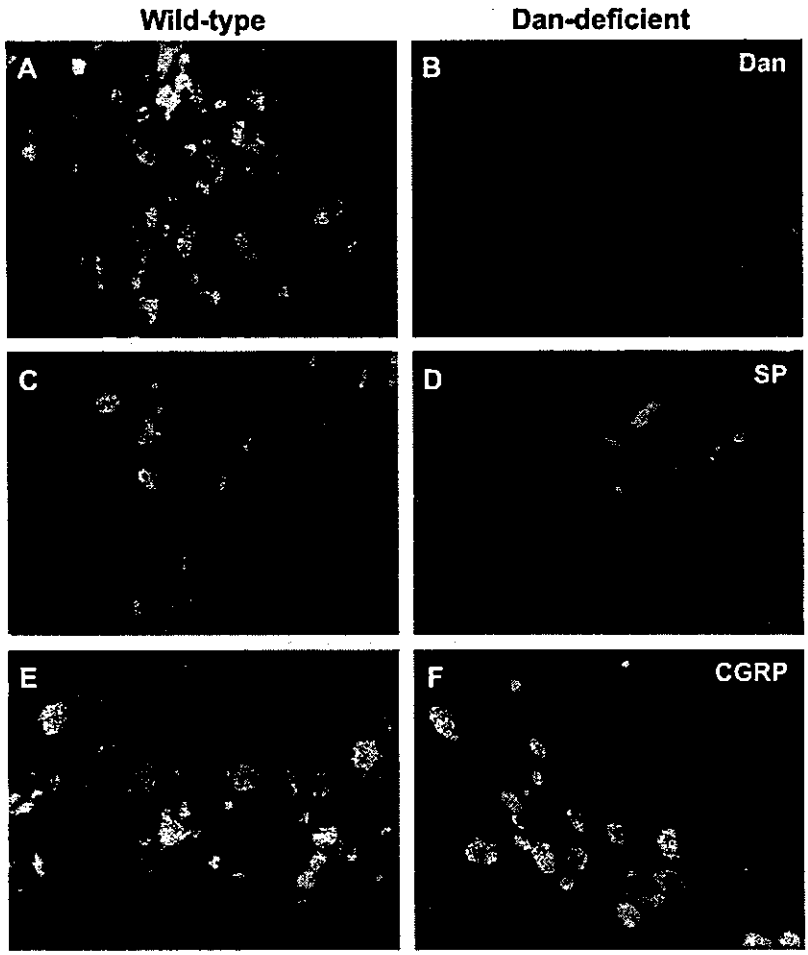

Fig. 2. Dan was absent in DRG neurons of Dan-deficient mice (B). DRG neurons derived from wild-type (A, C, and E) and Dan-deficient mice (B, D, and F) were reacted with antibody to Dan (A and B), substance P (SP) (C and D), or calcitonin gene-related peptide (CGRP) (E and F).

Dan-deficient, SP: 23 ± 5%; CGRP, 42 ± 7%) (mean ± SE) ($P > 0.1$). In the spinal dorsal horn of wild-type mice, Dan-IR sensory nerve terminals were observed in the inner part of lamina II, and SP- and CGRP-IR sensory nerve terminals were observed in laminae I and II (Fig. 3). NK1-IR neurons were detected mainly in laminae I and III. The patterns of SP-, CGRP-, and NK1-IR terminals in the spinal dorsal horn were not significantly different between wild-type and Dan-deficient mice.

Dan-IR nerve fibers were observed where a dorsal root lesion was made in wild-type mice (Fig. 3). Dan-IR free nerve endings were observed in the dermis of the footpads of wild-type mice, but not detectable in the skin of the footpads of Dan-deficient mice (Fig. 3). Two weeks after spinal nerve root section, the number of Dan-IR nerve terminals in the spinal dorsal horn decreased in wild-type mice. Because *Dan* mRNA was expressed in small DRG neurons (Ohtori et al., 2002), Dan was produced in small DRG neurons and seemed to be transported into the spinal dorsal horn and skin of footpads.

Dan immunoreactivity was seen in CGRP-, IB4-, and P2X3-IR neurons (Fig. 4). In all of the Dan-IR neurons, the ratios of Dan-IR neurons labeled with CGRP, IB4, or P2X3 were 33 ± 3%, 55 ± 9%, or 64 ± 8% (mean ± SE), respectively. On the other hand, some Dan was co-localized with NF200-IR myelinated A-fiber neurons (12 ± 3%). The ratios of Dan-IR neurons also labeled with CGRP, IB4, or P2X3 were significantly higher than that of neurons labeled with NF-200-IR ($P < 0.01$). Most of the double-labeled neurons were small-sized A-fiber neurons (Fig. 4).

Interestingly, Dan-IR nerve terminals in the spinal dorsal horn were located only in the inner part of lamina II. Interneurons in the inner part of lamina II differ considerably from those located dorsally in lamina I and in the outer part of lamina II. Immunocytochemical studies of the localization of the P2X3 receptor indicated its presence in a subpopulation of small-diameter non-peptidergic neurons that specifically bind IB4; these neurons project to (the inner part of) lamina II in the dorsal horn (Bradbury et al., 1998; Llewellyn-Smith and Burnstock, 1998). Dan-positive small DRG neurons stained with IB4 and P2X3 could project into the inner part of lamina II.

Almost all of the small DRG neurons were Dan-IR. In comparison, it has been reported that, respectively, only 20% and about 40% of small DRG neurons are substance P- and CGRP-containing (Neumann et al., 1996). In the current study, CGRP-IR DRG neurons were double-labeled with Dan. Non-IB4- and P2X3-IR Dan-positive DRG neurons were SP- or CGRP-containing small neurons projecting into lamina I and the outer layer of lamina II. However, it is unclear why Dan immunoreactivity in the spinal

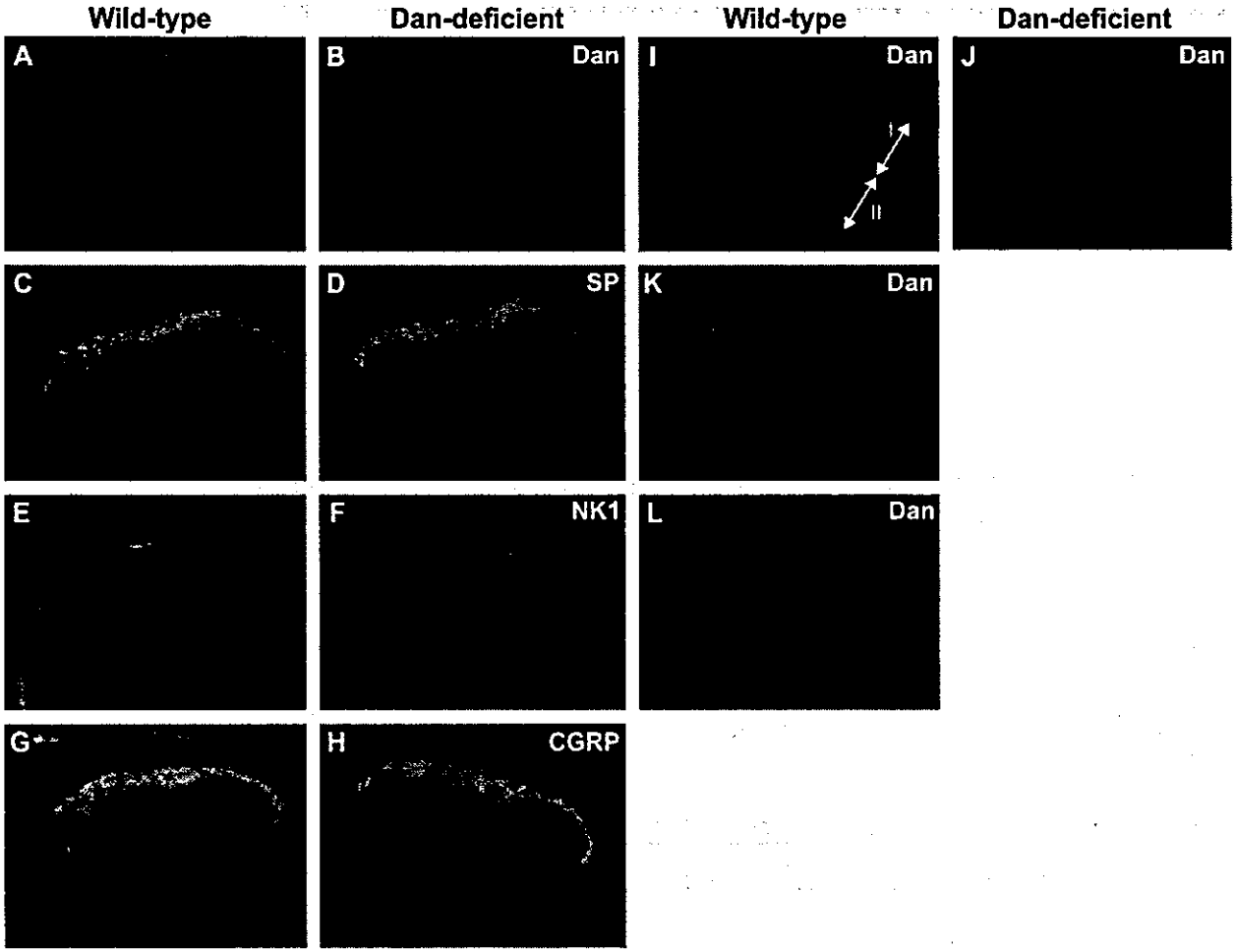

Fig. 3. In wild-type mice, DAN-IR sensory nerve terminals were observed in the inner part of lamina II, whereas Dan was absent in the spinal dorsal horn of Dan-deficient mice (B). In both types of mice, SP- (C and D) and CGRP-IR (G and H) sensory nerve terminals were detected in laminae I and II. Neurokinin receptor (NK1)-IR neurons were observed mainly in laminae I and III (E and F). Dan-IR sensory nerve endings in the dermis of footpads and sensory nerves in spinal dorsal root lesion were seen in wild-type mice (I and K), whereas they were not observed in the footpads of Dan-deficient mice (J). I, Epidermis; II, Dermis. Dan-IR nerve terminals in spinal dorsal horn decreased 2 weeks after dorsal root cut (L).

dorsal horn is seen only in the inner part of lamina II. One possible reason is that Dan protein in peptidergic neurons may not be transported to the central terminals in the spinal cord.

It has been reported that specific TGF-β family members are candidate regulators of CGRP expression in embryonic sensory neurons. BMPs 2, 4, and 6 stimulated CGRP expression in 60% of DRG neurons. BMP4 application supported maximal CGRP induction, suggesting that BMP4 is a "switch" rather than a continuous modulator of neuropeptide phenotype (Ai et al., 1999). In our study, we did not observe any differences in the distributions and ratios of SP- and CGRP-IR DRG neurons and sensory terminals in the spinal dorsal horn under physiological conditions. Dan seems not to regulate CGRP expression in embryonic and adult sensory neurons.

Thermal hypersensitivity and mechanical allodynia after inflammation

In the absence of inflammation or nerve injury, we found no differences in paw withdrawal responses to thermal and mechanical stimulation between Dan-deficient and wild-type mice. In wild-type and Dan-deficient mice, CFA injection produced a significant reduction in paw withdrawal latency to a heat stimulus on the injected side ($P < 0.01$) (Fig. 5A). Also, both types of mice displayed a significant mechanical allodynia ($P < 0.01$) (Fig. 5B). However, this decrease in the threshold of thermal and mechanical allodynia in Dan-deficient mice was significantly less than that of wild-type mice ($^*P < 0.05$). Injury to the sciatic nerve produced a significant decrease in the paw withdrawal threshold to thermal and von Frey hair stimulation on the injured side of wild-type ($P < 0.01$) and Dan-deficient mice ($P < 0.01$); however, the decrease in threshold between the two groups was not significantly different ($P > 0.1$) (Figs. 5C and D).

We previously showed that the Dan protein in rat DRG neurons increased only following CFA injection, but did not change following partial nerve injury. Furthermore, intrathecal injection of an antibody to Dan suppressed only inflammatory pain caused by the introduction of CFA and it did not suppress pain due to nerve injury (Ohtori et al., 2002).

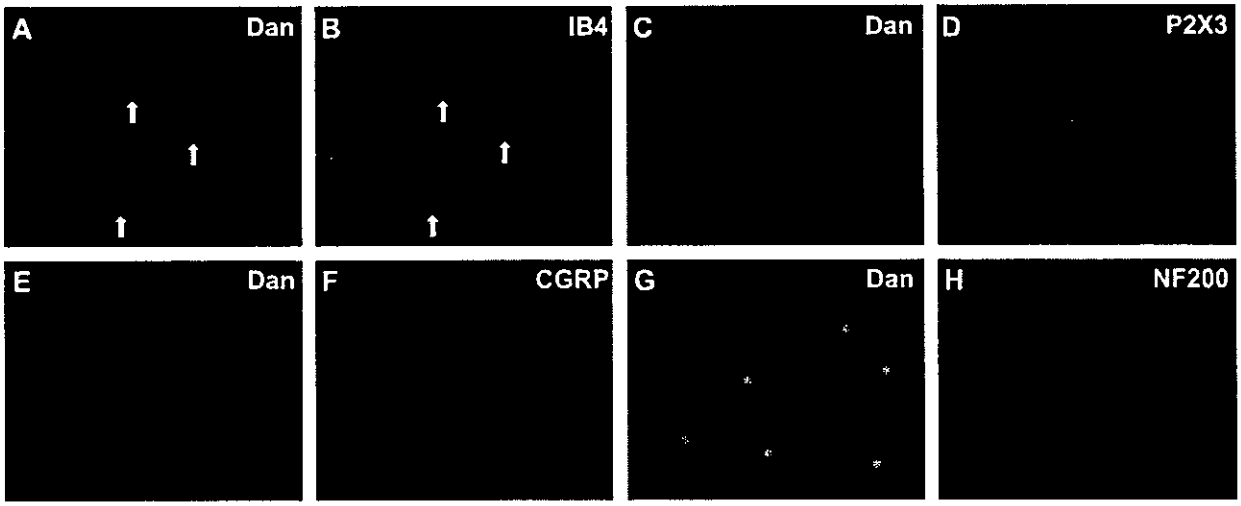

Fig. 4. Micrographs showing double-staining for Dan with isolectin B4 (IB4) (A and B), P2X3 (C and D), CGRP (E and F), or neurofilament 200 (NF200) (G and H). Dan was double-labeled with CGRP-IR DRG neurons. Dan immunoreactivity was seen in most IB4 and P2X3-IR neurons. On the other hand, most of Dan was not double-labeled in NF200-IR myelinated A-fiber neurons. Asterisks indicate Dan-IR and NF200-negative neurons.

It has also been reported that, in inflammatory models, SP and CGRP were increased in the dorsal root ganglia and the dorsal horn of the lumbar spinal cord (Donnerer et al., 1992; Noguchi and Ruda, 1992; Noguchi et al., 1988) and that the neurokinin receptor (NK1) was increased in the dorsal horn (Abbadie et al., 1996; McCarson and Krause, 1994).

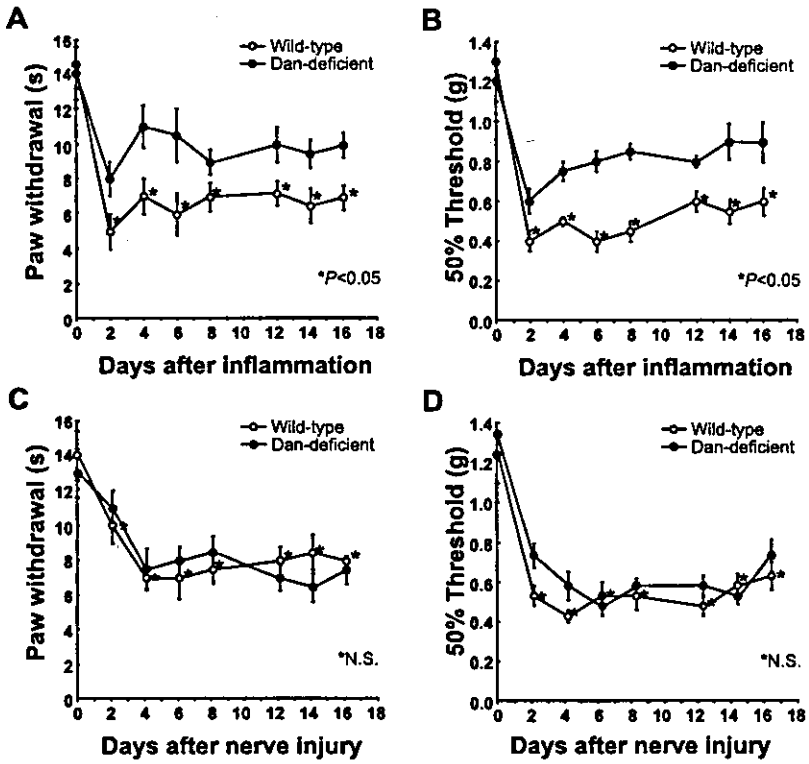

Fig. 5. Hyperalgesia measured by withdrawal to noxious thermal stimulation of the hind paw (A). The data are expressed as the difference in paw withdrawal latency between wild-type and Dan-deficient mice. After injection of CFA, significant reduction in paw withdrawal latency was observed in both types of mice; however, the decrease was significantly different between wild-type and Dan-deficient mice ($P < 0.05$). Inflammation also produced a significant decrease in paw withdrawal threshold (B). Asterisks indicate a significantly lower threshold on the inflammatory side in the wild-type mice compared with that of Dan-deficient mice ($P < 0.05$). Nerve injury also produced hyperalgesia measured by withdrawal to noxious thermal stimulation of the hind paw (C) and a significant decrease in the paw withdrawal threshold to von Frey filament stimulation (D). However, there were no differences between wild-type and Dan-deficient mice ($P > 0.1$).

Indeed, 4 days after inflammation in the current study, the fractions of SP- and CGRP-IR DRG neurons were 40 ± 4% (mean ± SE) and 52 ± 5%, respectively, in wild type and corresponding values for Dan-deficient mice were 31 ± 4% and 49 ± 5% (Figs. 6 and 7). The ratio of SP- and CGRP-IR neurons in both types of mice significantly increased compared with a non-inflammatory control ($P < 0.05$). The ratio of SP-IR neurons in wild-type mice was higher than that in Dan-deficient mice ($P < 0.05$) (Figs. 6 and 7); however, there was no significant difference in the ratio of CGRP-IR neurons in both types of mice after inflammation ($P > 0.1$). The relationship between Dan and other peptides influenced by neuropathic or inflammatory pain remains unclear. It is possible that Dan might induce SP in DRG neurons under inflammatory conditions.

Protein kinase C gamma (PKC) staining is also confined to interneurons of the inner part of lamina II. Mice that lack PKC displayed normal responses to acute pain stimuli, but they almost completely failed to develop a neuropathic pain syndrome after partial sciatic nerve section (Malmberg et al., 1997). On the other hand, the P2X3 receptor is important during inflammatory periods and may play a role in the modulation of spinal nociceptive transmission following the development of inflammation, but these receptors play at most a minor role in spinal nociceptive processing in normal and neuropathic animals (Liu and Tracey, 2000; Stanfa et al., 2000). Dan, which was expressed in the inner part of lamina II, seems to regulate only inflammatory pain.

Depression of Fos expression in inflammatory pain

Fos-IR neurons were present mainly in the left dorsal horn (Figs. 8 and 9). The time course of Fos expression following CFA injection in wild-type and Dan-deficient mice is shown in Fig. 10. The numbers of Fos-IR neurons following CFA injection in the superficial and deep laminae of Dan-deficient mice were significantly less than those in wild-type mice ($P < 0.05$) (Fig. 11A). The amount of Fos expression in lamina II of Dan-deficient mice was significantly less than that in wild-type mice ($P < 0.05$) (Fig. 11C). The difference was detected for all the periods we observed

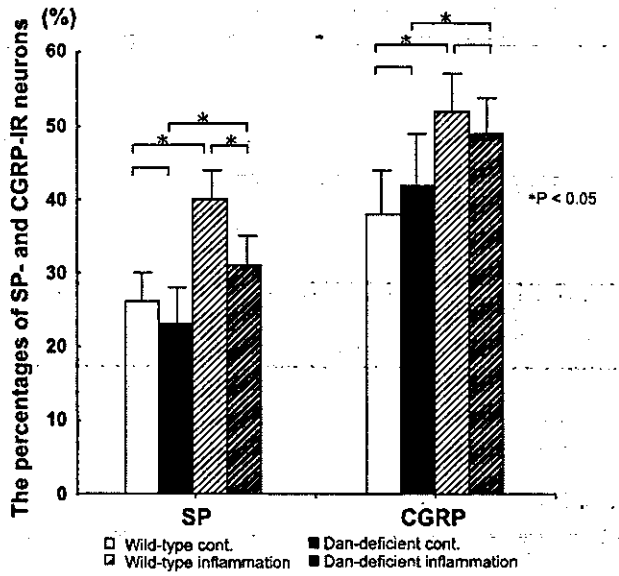

Fig. 7. The percentages of SP- and CGRP-IR DRG neurons were not significantly different between wild-type and Dan-deficient mice under normal conditions (day 0; wild type, SP: 26 ± 4%, CGRP, 38 ± 6%; Dan-deficient, SP: 23 ± 5%, CGRP, 42 ± 7%) (mean ± SE) ($P > 0.1$). Four days after inflammation, the ratios of SP- and CGRP-IR neurons in both types of mice were significantly increased compared with non-inflammatory control ($P < 0.05$). The ratio of SP-IR neurons in wild-type mice was higher than that in Dan-deficient mice ($P < 0.05$). However, there was no significant difference in the ratio of CGRP-IR neurons in both types of mice after inflammation ($P > 0.1$).

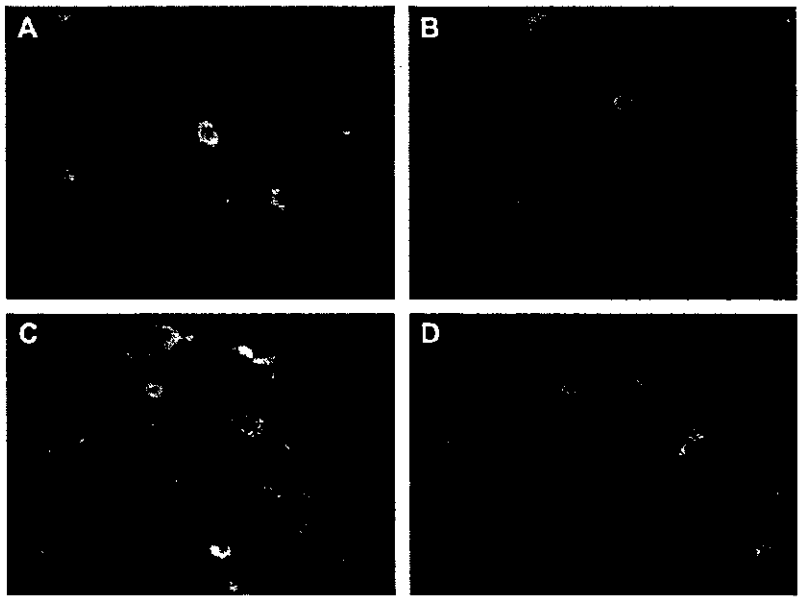

Fig. 6. Change in ratio of SP-IR DRG neurons of wild type (A, control group; C, inflammatory group) and Dan-deficient (B, control group; D, inflammatory group) mice after inflammation. SP was increased in wild-type and Dan-deficient mice after inflammation (C and D), however the number of SP-IR DRG neurons in wild-type mice (C) was significantly higher than that in Dan-deficient mice (D).

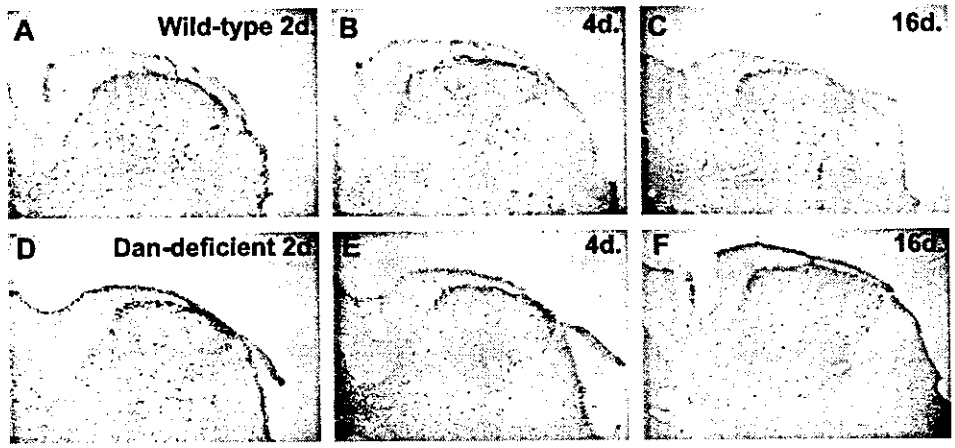

Fig. 8. Inflammation-induced Fos expression in the spinal dorsal horn in wild-type (A, B, and C) and Dan-deficient mice (D, E, and F). Fos-IR neurons in the superficial and deep laminae were observed at days 2 (A and D), 4 (B and E), and 16 (C and F) after CFA injection into the hind paw. More neurons were stained in wild-type mice than in Dan-deficient mice.

(Fig. 11). The amount of Fos expression in lamina I and II, 4 days after inflammation, was depressed by intrathecal injection of Dan antibody in wild-type mice ($P < 0.05$) (Figs. 10 and 11D). However, in the partial nerve injury models, the numbers of Fos-IR neurons following nerve injury in the superficial and deep laminae of Dan-deficient mice were not significantly different from those in wild-type mice ($P > 0.1$) (Fig. 11B).

It has been reported that noxious chemical and thermal stimulation of the skin leads to Fos expression in spinal dorsal horn neurons (Hunt et al., 1987). An increase of Fos expression in the spinal cord is observed following nerve injury in animal models (Catheline et al., 1999; Chi et al., 1993; Dai et al., 2001; Hudspith et al., 1999). The increase of Fos in the superficial and deep laminae may be related to hypersensitivity to noxious and innocuous stimuli following nerve injury (Catheline et al., 1999; Dai et al., 2001). After inflammation of the rat hind paw, noxious and innocuous stimuli induced a significantly large increase in Fos expression by dorsal horn neurons in laminae I–VI during lasting peripheral inflammation (Ma and Woolf, 1996).

In the current study, Fos expression was observed in superficial and deep laminae in the inflammatory and nerve injury models. We observed the same pattern, period, and location of spinal dorsal horn Fos expression as previously reported. Dan-deficient mice did not show significant hypersensitivity and mechanical allodynia caused by inflammation when compared with wild-type mice. However, the Dan-deficient mice showed hypersensitivity and mechanical allodynia caused by nerve injury. This finding was correlated with the decreased Fos expression observed in Dan-deficient mice under inflammatory conditions and with an insignificant difference in Fos expression after nerve injury when compared with wild-type mice.

Because Dan-IR nerve terminals were in the inner part of lamina II, the localization of Dan may lead to depression of Fos expression only in the inner part of lamina II in Dan-deficient mice. However, Fos expression was decreased in all superficial and deep laminae in the spinal dorsal horn. We postulate that the reason for this is as follows: it has been reported that NK1 receptor-immunoreactive neurons with cell bodies in lamina III or IV and dendrites that enter the superficial laminae also receive dense synaptic innervation from SP primary afferents (Todd et al., 2002). After inflammation of rat hind paw, Fos expression is more common in neurons with NK1 receptors. Therefore, a significant

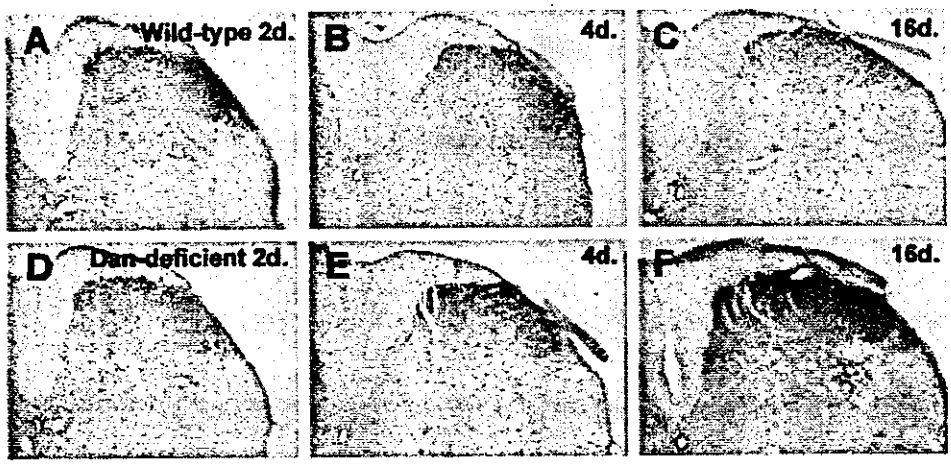

Fig. 9. Fos expression after nerve ligation in the spinal dorsal horn in wild-type (A, B, and C) and Dan-deficient mice (D, E, and F). The number of Fos-IR neurons at days 2 (A and D), 4 (B and E), and 16 (C and F) after nerve ligation was not significantly different between wild-type and Dan-deficient mice.

Fig. 10. Effect of intrathecally administered Dan monoclonal antibody on a CFA model of wild-type mice 4 days after inflammation. The level of Fos expression in superficial and deep layers 2 h after stimulation was depressed by intrathecal injection of Dan antibody in wild-type mice. (A, administration of mouse IgG; B, administration of Dan antibody).

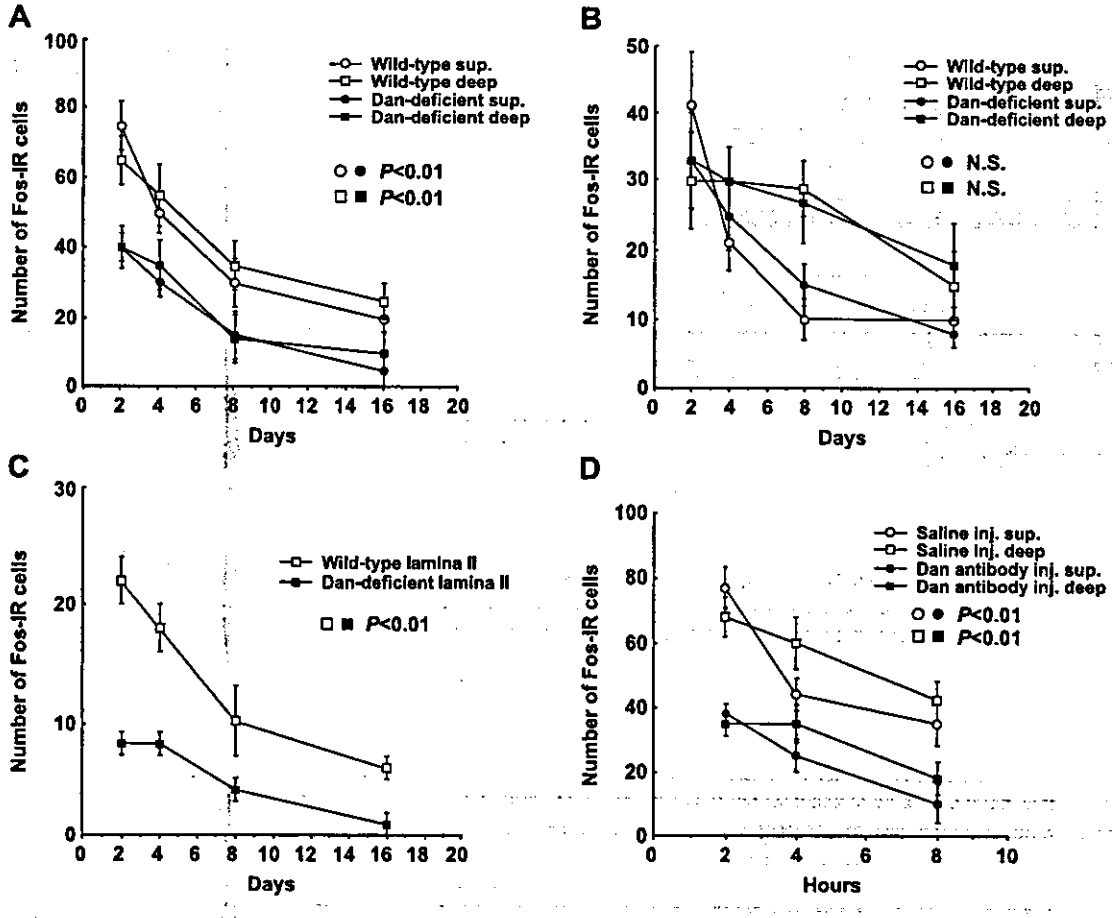

Fig. 11. Time course of Fos expression caused by inflammation in wild-type (open symbols) and Dan-deficient mice (solid symbols) (A). The numbers of Fos-IR cells in both laminae were less in Dan-deficient mice than in wild-type mice at all periods we observed ($P < 0.01$). In lamina II, immunoreacted for Dan, the number of Fos-IR cells was less in Dan-deficient mice (open square) than in wild-type mice (solid square) ($P < 0.01$) (C). Stimulation of the hind paw produced Fos in wild-type and Dan-deficient mice after nerve injury (B). On days 2, 4, 8, and 16, we did not observe significant differences in the numbers of Fos-IR cells in the superficial and deep laminae between both types of mice (open circle, wild-type superficial; open square, wild-type deep; solid circle, Dan-deficient superficial; solid square, Dan-deficient deep) ($P > 0.1$). The amount of Fos expression in superficial and deep layers 4 days after inflammation was depressed by intrathecal injection of Dan antibody in wild-type mice ($P < 0.05$) (Fig. 8D). Each point represents the time after stimulation of footpads (open circle, Fos expression in the superficial layers after IgG administration; open square, Fos expression in the deep layers after IgG administration; solid circle, Fos expression in the superficial layers after Dan-antibody administration; solid square, Fos expression in the deep layers after Dan-antibody administration).

proportion of these cell bodies in deep layers would be excited by noxious stimulation (Todd et al., 2002). SP was increased in the dorsal root ganglia, and the amount of these peptides in projections from the dorsal horn of the lumbar spinal cord would also be increased in inflammatory models (Schaible et al., 1994; Neumann et al., 1996; Noguchi et al., 1995). In the process, Dan is related to SP induction in DRG neurons after inflammation in the current study. We did not examine Dan receptors in the spinal cord. However, intrathecal-administered Dan suppressed pain behavior and Fos expression in superficial and deep layers of the spinal cord. We therefore propose that, except for SP induction in DRG, Dan also stimulates Fos in Dan-immunoreactive cells in the deep layer via the Dan-receptor pathway.

Experimental methods

The protocols for animal procedures in these experiments followed National Institutes of Health guidelines for the Care and Use of Laboratory Animals (1996 revision) and received approval from the ethics committees of our institutions.

Generation of Dan-deficient mice

A radio-labeled full-length mouse *Dan* cDNA was used to screen a mouse genomic library (λFIXII) by standard procedures. Genomic clones that gave a positive signal in the initial screening were digested with various combinations of restriction enzymes to verify that rearrangements had not occurred. The targeting construct was generated by replacing a 2.5-kb *Eco*RI–*Sma*I restriction fragment containing the exons II and III with an MC1-Neo cassette. An MC1-DT-A cassette was then inserted into the 3′side of the Neo cassette for negative selection. Forty micrograms of the linearized targeting vector were electroporated into 6×10^6 R1 ES cells, and the transfected cells were maintained in the presence of G418. Genomic DNA was prepared from the G418-resistant clones and subjected to Southern analysis using a radiolabeled *Sma*I–*Xba*I restriction fragment as a probe. Of 240 clones analyzed, two clones carried the desired mutant allele. These two targeted ES cell clones were then injected into BDF1 blastocysts to generate chimeric mice. Chimeras were mated with C57BL/6 females and lines were maintained by backcross onto C57BL/6 females.

Genotyping of mice at the Dan locus

Animals were genotyped either by Southern blot hybridization or by PCR-based analysis. For Southern analysis, mouse genomic DNA was digested completely with *Bam*HI, separated by 0.8% agarose gel electrophoresis, and transferred onto a nylon membrane filter. The filter was probed with the radiolabeled *Sma*I–*Xba*I restriction fragment. This strategy identified a 13-kb wild-type allele or a 1-kb targeted allele. PCR analysis was performed with the following primers: forward-1 (f1), 5′-ATACCTGCTTCCCCACTCCT-3′, reverse-1 (r1), 5′-GAACCTGCGTGCAATCCATCTT-3′; and forward-2 (f2), 5′-GACAAGAGTGCCTGGTGTGA-3′, reverse-2 (r2), 5′-GTGTTGGGGACGCTGTAACT-3′, which resulted in a 458-bp mutant type and a 227-bp wild-type product, respectively. The cycling conditions were 2 min at 98°C and 35 cycles of 30 s at 98°C, 30 s at 62°C, and 30 s at 72°C.

Inflammation model and nerve injury model

Forty-eight 12-week-old male Dan-deficient and wild-type mice were used. Under anesthesia with sodium pentobarbital (40 mg/kg, ip), 20 μl of complete Freund's adjuvant (CFA; 50 μg *Mycobacterium butyricum* in an oil-in-saline emulsion; Sigma, St. Louis, MO) was injected into the left hind paw. Partial sciatic nerve injury was caused by tight ligation of one-third to one-half of the left sciatic nerve.

Behavioral testing

The latency of paw withdrawal to thermal stimuli was measured as has been previously described (Hargreaves et al., 1988). Wild-type and Dan-deficient mice were placed in a planter test apparatus (UGO Basile; Camerio, Italy) consisting of a radiant heat source below an elevated floor of transparent glass. The radiant heat source beneath the glass floor was turned on, and the time between the start of stimulation and hind paw withdrawal was measured five times every 10 min. The average time for hind paw withdrawal was recorded. The level of tactile allodynia was estimated from 50% probability thresholds for paw withdrawal from mechanical stimuli using von Frey hairs, as previously described (Chaplan et al., 1994).

Time course of Fos expression in CFA and nerve injury models

Touch-evoked increases in Fos expression were examined from 2 to 16 days after CFA injection or nerve injury to wild-type (n = 24) and Dan-deficient mice (n = 24). Gentle touch stimuli were applied manually to the injected plantar surface of these animals with the flat surface of the experimenter's thumb, as described in detail previously (Sivilotti and Woolf, 1994). Each touch, lasting 2 s and moving from the middle position of the foot to the distal footpad, was applied once every 4 s for 10 min under halothane anesthesia.

We examined the effect of intrathecally administered mouse monoclonal antibody to Dan (5 μg) (Chiba Cancer Center Research Institute) on the CFA model in wild-type mice 4 days after inflammation (n = 12). To administer antibodies intrathecally, a 30-gauge needle was inserted into the intralamina space between L6 and S1. Stimulation of the footpad was applied after intrathecal injection of Dan antibody. To obtain control data, 5 μg of mouse IgG_1 was administered (n = 12). The number of Fos-immunoreactive (IR) cells in the spinal cord was evaluated 2, 4, and 8 h after stimulation.

Immunohistochemistry

Mice were anesthetized with 3% halothane and perfused transcardially with 100 ml of 4% paraformaldehyde (PFA) in phosphate buffer (0.1 M, pH 7.4). The spinal cord was resected at the level of C4 and L5, and the L5 dorsal root ganglia (DRGs) and footpad were removed and 20-μm sections cut on a cryostat. To examine axonal transport of Dan from DRG to the spinal dorsal horn, the spinal cord at the level of L4 was resected 2 weeks after dorsal root section. Sections were incubated in a blocking solution containing 0.3% Triton X-100 and 5% skim milk in 0.01 M phosphate-buffered saline (PBS) for 90 min at room temperature. Sections were processed immunohistochemically using a free-floating avidin–biotin complex (ABC) technique by incubating them with rabbit antibody to Dan (1:1000 in blocking solution), substance P